# CENTRIFUGAL STRESS IN CONICAL ROTORS AND ROTORS OF ARBITRARY CROSS SECTION

ROBERT L. HARSHBERGER
and
DARRELL CLINTON TROUTMAN

# CENTRIFUGAL STRESS IN CONICAL ROTORS AND ROTORS OF ARBITRARY CROSS SECTION

by

Robert Lee Harshberger
Lieutenant, United States Navy
B.S., United States Naval Academy, 1958

and

Darrell Clinton Troutman
Lieutenant, United States Navy
B.S., United States Naval Academy, 1958

Submitted in partial fulfillment
of the requirements
for the degree of

MASTER OF SCIENCE IN AERONAUTICAL ENGINEERING

from the

UNITED STATES NAVAL POSTGRADUATE SCHOOL
May 1966

## ABSTRACT

Part I of this report evaluates a computer solution for the centrifugal stresses in rotors of arbitrary cross section, as proposed by Lt. R. A. Johnson in 1965. This solution was found to be unstable and in its present form is unacceptable.

Part II is an evaluation of the hot spin test unit of the United States Naval Postgraduate School. This facility was found capable of measuring centrifugal strains with excellent accuracy.

Part III presents a new and original analytical solution for the stresses in any conical rotor of constant thickness. The theoretically predicted stresses are found to be in close agreement with the measured values for the particular rotor tested.

TABLE OF CONTENTS

LIST OF ILLUSTRATIONS

## TABLE OF SYMBOLS AND ABBREVIATIONS

| | |
|---|---|
| $\rho$ | Mass density of rotor material, (lb.sec.$^2$/in.$^4$) |
| $\sigma_r$ | Radial stress, (lb./sq. in.) |
| $\sigma_\theta$ | Tangential stress, (lb./sq. in.) |
| $\sigma_z$ | Axial stress, (lb./sq. in.) |
| $\omega$ | Angular velocity, (rad./sec.) |
| r | Radial coordinate ---- Radial distance, (in.) |
| $\Theta$ | Tangential coordinate ---- Angle between vertical and $r_o$ |
| z | Axial coordinate ---- Axial distance, (in.) |
| $\Phi$ | Airy's stress function |
| $\nu$ | Poisson's ratio |
| $\nabla$ | Differential operator |
| $r_o$ | Radial distance to assumed load, (in.) |
| $z_o$ | Axial distance to assumed load, (in.) |
| R | Radial distance from rotor periphery point to point of assumed load, (in.) ---- Maximum radius, (in.) |
| n | $n^{th}$ point station on the rotor periphery |
| m | $m^{th}$ point station on the imaginary boundary |
| P | Axial load parameter |
| Q | Radial load parameter |
| $\sigma_{r_{nm}}^{(P)}$ | The radial stress at point n caused by an axial load P applied at imaginary point m |
| $\sigma_{r_{n_{PART}}}$ | The radial stress at point n obtained from the particular solution |
| $\sigma_{r_{n_{B.C.}}}$ | The known radial stress at point n associated with boundary conditions |
| E | Modulus of elasticity, (psi) |

$G$ Modulus of rigidity, (psi)

$\Delta V$ Recorder reading, (millivolts)

$\epsilon$ Strain, (microinches/inch)

G.F. Gage factor

$V_c$ Impressed circuit voltage, (volts)

$T_r$ Distributed force in radial direction, (lb./in.)

$T_\theta$ Distributed force in tangential direction, (lb./in.)

$M_r$ Distributed radial bending moment, (in.lb./in.)

$M_\theta$ Distributed tangential bending moment, (in.lb./in.)

$h$ Thickness of disk with respect to the z axis, (in.)

$\bar{h}$ Axial distance to centroid of disk, (in.)

$u_r$ Radial displacement of centroid

$\Phi$ Angle of rotation of centroid

$\Psi$ Stress function

$\chi$ Stress function

$\alpha$ Cone angle

$\sigma_{r_d}$ Direct radial stress

$\sigma_{r_b}$ Bending radial stress

## SUMMARY

Current aeronautical and space engineering technology has shown a requirement for light weight, high speed, rotating components. Unsymmetrical heating may induce an undesirable stress distribution in these rotors. It is possible that a rotor which is designed to be unsymmetrical in the plane normal to the axis of rotation, can be used to alter favorably this stress pattern. Furthermore, design restrictions may require utilizing a rotor which has no plane of symmetry normal to the axis of rotation.

Prediction of centrifugal and thermal stresses of these rotating components having arbitrary cross section has been a difficult problem, based essentially on approximate methods. A more accurate analytical solution is desirable. Additionally, more accurate methods of measuring the stresses developed in such rotors would be advantageous.

This paper presents investigations undertaken to accomplish both of the above stated objectives. It consists of three parts. The first part is the expansion and evaluation of a proposed theoretical solution for the centrifugal elastic stresses in a rotor of arbitrary and unsymmetrical cross section. A computer formulation of this solution was developed by Lieutenant Robert A. Johnson in 1965. Further investigation of this solution was conducted by the current authors. Application of the method to the limiting case of a symmetrical flat disk suggested that the theory was sound. However, computer analysis of shapes other than

the above were unsatisfactory. The results indicated that the computer program, which requires the simultaneous solution of a large number of equations, is extremely sensitive to rotor contour and is inherently unstable. Further investigation is required to determine the nature of this instability and possible means of eliminating it.

The second part of this paper is an evaluation of the hot spin test facilities of the United States Naval Postgraduate School. An experimental investigation was conducted to determine the strain measuring capabilities of this recently acquired unit.

Two slip ring assemblies were supplied with this facility. The first of these is air cooled and has intermittant brush contact. The second has freon cooling and continuous brush contact. Utilization of the air-cooled unit proved unsatisfactory. The difficulty was associated with the method of connecting the slip ring and strain gage wiring. With the second assembly installed, satisfactory results were obtained.

A flat disk test rotor was fabricated and utilized to evaluate the unit. The induced strains in this rotor were measured. These were converted to stresses and the results compared to the known theoretical solution. Agreement was good. The amount of data scatter was slight. The standard deviation of strain was estimated to be 15 micro-inches per inch.

To provide experimental verification of the theoretical solution for the stresses in unsymmetrical rotors, a coned

rotor of constant thickness was fabricated and tested. Part III of this report presents the results of these tests, and an exact analytical solution for the stresses in any coned rotor. This solution was made necessary by failure of Part I to give the expected results.

The solution shows that the stress distribution is essentially determined by a single parameter, which depends on the geometry of the disk. The stresses at any point are fixed by a set of non-dimensional functions. These functions can be tabulated once and for all, whereupon the stresses in any conical rotor of constant thickness can be found without the necessity of using a computer.

For the specific rotor tested, analytical and measured stresses compared favorably. The stresses of the middle surface were found to be generally less than in a symmetrical disk. However, large surface stresses were induced, with considerable stress variation across the thickness.

This investigation has demonstrated that the hot spin unit is capable of making accurate strain measurements. This capability should be fully exploited. While the goal of predicting the stresses in a rotor of arbitrary cross section has not yet been reached, the exact solution for the centrifugal stresses in coned rotors is believed to be a significant contribution towards attaining this goal.

# PART I: STRESSES IN ROTORS OF ARBITRARY CROSS SECTION

## INTRODUCTION

This section of this report is concerned with the stress analysis of rotating shapes having no plane of symmetry normal to the axis of rotation. An attempt to obtain an analytical solution for the centrifugal elastic stresses in a rotor of arbitrary and unsymmetrical cross section was initiated by Lieutenant Robert A. Johnson, [1], at the United States Naval Postgraduate School, Monterey, California in 1965. Due to time limitations the proposed computerized solution was not completed. The present paper includes an expansion of Lt. Johnson's investigation and an evaluation of the results obtained.

The method chosen to evaluate this solution was comparison of computer results with the known solution for the limiting case of a symmetrical rotating disk. These results indicated that the theoretical solution was essentially sound. However, computer results for other shapes was unsatisfactory.

## ANALYSIS

The following is a synopsis of the proposed analytical solution [1] for the centrifugal elastic stresses in a rotating disk of arbitrary cross section. Where required, this solution has been corrected by the current authors.

The usual assumption of linearity between stress and strain is adopted in this study. The rotor is homogeneous. Variations of physical properties with temperature might well be significant but are neglected in the present investigation.

For the proposed rotor of arbitrary cross section, rotating at a constant angular velocity ($\omega$), as in Fig. 1, the governing differential equations of equilibrium in cylindrical coordinates are

$$\frac{\partial \sigma_r}{\partial r} + \frac{\partial \tau_{rz}}{\partial z} + \frac{\sigma_r - \sigma_\theta}{r} + \rho \omega^2 r = 0$$

$$\frac{\partial \tau_{rz}}{\partial r} + \frac{\partial \sigma_z}{\partial z} + \frac{\tau_{rz}}{r} = 0 \qquad (1\text{-}1)$$

By assuming a stress function, $\Phi$, in the form of polynomials a particular solution to equations (1-1) is found to be

$$\sigma_r = -\frac{\rho\omega^2}{3} r^2 - \frac{\rho\omega^2(1+3\nu)(1+\nu)}{6\nu(1-\nu)} z^2$$

$$\sigma_z = \frac{\rho\omega^2(1+3\nu)}{6\nu} r^2 \qquad (1\text{-}2)$$

$$\sigma_\theta = -\frac{\rho\omega^2(1+3\nu)(1+\nu)}{6\nu(1-\nu)} z^2$$

$$\tau_{rz} = 0$$

To define completely the stresses in the rotor being considered, it is necessary to determine a complementary solution to equations (1-1). Assuming such a solution is found, superposition of it and the particular solution, and utilization of the appropriate boundary conditions, will yield the stresses at all points of the body.

For the complementary solution, the equations of equilibrium reduce to

$$\frac{\partial \sigma_r}{\partial r} + \frac{\partial \tau_{rz}}{\partial z} + \frac{\sigma_r - \sigma_\theta}{r} = 0$$
$$\frac{\partial \tau_{rz}}{\partial r} + \frac{\partial \sigma_z}{\partial z} + \frac{\tau_{rz}}{r} = 0 \qquad (1\text{-}3)$$

Utilizing the concept of a stress function, $\Phi$, equations (1-3) are identically satisfied by placing

$$\sigma_r = \frac{\partial}{\partial z}\left(\nu \nabla^2 \Phi - \frac{\partial^2 \Phi}{\partial r^2}\right)$$
$$\sigma_\theta = \frac{\partial}{\partial z}\left(\nu \nabla^2 \Phi - \frac{1}{r}\frac{\partial \Phi}{\partial r}\right)$$
$$\sigma_z = \frac{\partial}{\partial z}\left[(2-\nu)\nabla^2 \Phi - \frac{\partial^2 \Phi}{\partial z^2}\right] \qquad (1\text{-}4)$$
$$\tau_{rz} = \frac{\partial}{\partial r}\left[(1-\nu)\nabla^2 \Phi - \frac{\partial^2 \Phi}{\partial z^2}\right]$$

It can be shown [2] that compatibility of strains requires in addition that the stress function satisfy the equation

$$\nabla^4 \Phi = 0 \qquad (1\text{-}5)$$

Since equation (1-5) is linear, the required complementary solution can be expressed in the form of a linear combination of judiciously chosen stress functions. Each

of these must individually satisfy equations (1-4) and (1-5). The amplitudes of the selected stress functions are determined so as to satisfy appropriate boundary conditions at selected points on the rotor periphery. To satisfy these boundary conditions, it is assumed that a series of axial and radial loads are applied along a control contour, that is, an imaginary boundary located at a finite distance from the actual rotor surface, Fig. 1. Each of these assumed loads has associated with it a stress distribution and corresponding stress function. The stress distributions corresponding to the assumed axial and radial ring loads of unit intensity are unknown but may be found.

To obtain the stress components for the above loads, the known results for a simple concentrated load [2] are utilized. This concept of a unit concentrated load is expanded into a series of infinitesimal loads uniformly distributed along a ring. Integration around the complete periphery yields the final stress components for each unit axial and radial ring load.

In Fig. 1, the stress components associated with the ring loads applied at a particular point (m) of the control contour, affect all points on the rotor surface. Conversely, the stresses induced at some point (n) on the rotor surface include effects from all points of assumed load application. In integral form, the final stress components at any rotor surface point (n) due to application of a unit <u>axial</u> load at point (m), are found to be

$$\sigma_r = \frac{1}{4\pi(1-\nu)r_o^2}\int_0^{\pi}\frac{z-z_o}{r_o}\left\{\frac{(1-2\nu)}{\left(\frac{R}{r_o}\right)^3} - \frac{3\left(\frac{r}{r_o}-\cos\theta\right)^2}{\left(\frac{R}{r_o}\right)^5}\right\}d\theta$$

$$\sigma_\theta = \frac{1}{4\pi(1-\nu)r_o^2}\int_0^{\pi}\frac{z-z_o}{r_o}\left\{\frac{(1-2\nu)}{\left(\frac{R}{r_o}\right)^3} - \frac{3\sin^2\theta}{\left(\frac{R}{r_o}\right)^5}\right\}d\theta$$

$$\sigma_z = -\frac{1}{4\pi(1-\nu)r_o^2}\int_0^{\pi}\frac{z-z_o}{r_o}\left\{\frac{(1-2\nu)}{\left(\frac{R}{r_o}\right)^3} + \frac{3\left(\frac{z-z_o}{r_o}\right)^2}{\left(\frac{R}{r_o}\right)^5}\right\}d\theta \qquad (1\text{-}6)$$

$$\tau_{rz} = -\frac{1}{4\pi(1-\nu)r_o^2}\int_0^{\pi}\left\{\left[\frac{(1-2\nu)}{\left(\frac{R}{r_o}\right)^3} + \frac{3\left(\frac{z-z_o}{r_o}\right)^2}{\left(\frac{R}{r_o}\right)^5}\right]\left[\frac{r}{r_o}-\cos\theta\right]\right\}d\theta$$

where

$$\left(\frac{R}{r}\right)^2 = 1 + \left(\frac{r}{r_o}\right)^2 - 2\left(\frac{r}{r_o}\right)\cos\theta + \left(\frac{z-z_o}{r_o}\right)^2$$

The final stress components at any rotor surface point (n) due to application of a unit <u>radial</u> load at point (m) are of a similar nature and are as shown in [1]. The eight resulting integrals can be evaluated by computer for any assigned values of the arguments $(r/r_o)$ and $(z-z_o)/r_o$. Note that $r_o, z_o$ are the coordinates of the ring load (m) on the control contour, and r,z are the coordinates of the point (n) where the stresses are being evaluated. Hence the arguments $(r/r_o)$ and $(z-z_o)/r_o$ merely express the location of the point (n) with respect to the ring load at (m). These integral functions are essentially influence coefficients which express in generalized terms the stresses at (n) produced by unit loads acting at (m).

Utilizing Mohr's circle relationships, solutions to equations (1-6) are converted into normal stresses, $\sigma_N$ , and tangential stresses, $\tau_T$ , at each point (n) on the rotor surface. The resulting boundary stress equations become of the form

$$\sigma_{N_n} = \sum_{m=1}^{K} \left\{ P_m \overset{(P)}{\sigma_{N_m}} + Q_m \overset{(Q)}{\sigma_{N_m}} \right\}$$
$$\tau_{T_n} = \sum_{m=1}^{K} \left\{ P_m \overset{(P)}{\tau_{T_m}} + Q_m \overset{(Q)}{\tau_{T_m}} \right\} \qquad (1\text{-}7)$$

where the unit axial and radial loads applied at each point (m) are to be multiplied by undetermined amplitudes $P_m$ and $Q_m$, and where superscripts P and Q are used to represent axial and radial ring loads respectively.

This complementary solution is to be superimposed upon the particular solution for the radial and tangential stresses at each point (n). These are obtained by applying Mohr's circle relationships to equations (1-2). This combination is then set equal to the known boundary stresses and thereby defines the solution for the unknown coefficients $P_m$ and $Q_m$.

To solve for these unknown coefficients, a stress matrix consisting of $2 \cdot k$ equations must be solved, where k represents the number of assumed points of load application. This stress matrix is of the form

$$\begin{aligned}
&P_1 \overset{(P)}{\sigma_{N_{11}}} + P_2 \overset{(P)}{\sigma_{N_{12}}} + \cdots P_K \overset{(P)}{\sigma_{N_{1K}}} + Q_1 \overset{(Q)}{\sigma_{N_{11}}} + Q_2 \overset{(Q)}{\sigma_{N_{12}}} + \cdots Q_K \overset{(Q)}{\sigma_{N_{1K}}} + \sigma_{N_{1\,PART}} = \sigma_{N_{1\,B.C.}} \\
&P_1 \overset{(P)}{\tau_{T_{11}}} + P_2 \overset{(P)}{\tau_{T_{12}}} + \cdots P_K \overset{(P)}{\tau_{T_{1K}}} + Q_1 \overset{(Q)}{\tau_{T_{11}}} + Q_2 \overset{(Q)}{\tau_{T_{12}}} + \cdots Q_K \overset{(Q)}{\tau_{T_{1K}}} + \tau_{T_{1\,PART}} = \tau_{T_{1\,B.C.}} \qquad (1\text{-}8) \\
&P_1 \overset{(P)}{\sigma_{N_{21}}} + P_2 \overset{(P)}{\sigma_{N_{22}}} + \cdots P_K \overset{(P)}{\sigma_{N_{2K}}} + Q_1 \overset{(Q)}{\sigma_{N_{21}}} + Q_2 \overset{(Q)}{\sigma_{N_{22}}} + \cdots Q_K \overset{(Q)}{\sigma_{N_{2K}}} + \sigma_{N_{2\,PART}} = \sigma_{N_{2\,B.C.}}
\end{aligned}$$

$$
\begin{aligned}
&P_1 \overset{(P)}{\sigma}_{N_{K1}} + \cdots\cdots P_K \overset{(P)}{\sigma}_{N_{KK}} + Q_1 \overset{(Q)}{\sigma}_{N_{K1}} + \cdots\cdots Q_K \overset{(Q)}{\sigma}_{N_{KK}} + \sigma_{N_{K_{PART}}} = \sigma_{N_{K_{B.C}}} \\
&P_1 \overset{(P)}{\tau}_{T_{K1}} + \cdots\cdots P_K \overset{(P)}{\tau}_{T_{KK}} + Q_1 \overset{(Q)}{\tau}_{T_{K1}} + \cdots\cdots Q_K \overset{(Q)}{\tau}_{T_{KK}} + \tau_{T_{K_{PART}}} = \tau_{T_{K_{B.C}}}
\end{aligned}
\tag{1-8}
$$

When the solution to this matrix is found, the coefficients may be substituted into the following equations to yield the stresses desired. Thus

$$
\begin{aligned}
\sigma_{r_n} &= \sum_{m=1}^{K} \left\{ P_m \overset{(P)}{\sigma}_{r_{nm}} + Q_m \overset{(Q)}{\sigma}_{r_{nm}} \right\} + \sigma_{r_{n_{PART}}} \\
\sigma_{\theta_n} &= \sum_{m=1}^{K} \left\{ P_m \overset{(P)}{\sigma}_{\theta_{nm}} + Q_m \overset{(Q)}{\sigma}_{\theta_{nm}} \right\} + \sigma_{\theta_{n_{PART}}} \\
\sigma_{z_n} &= \sum_{m=1}^{K} \left\{ P_m \overset{(P)}{\sigma}_{z_{nm}} + Q_m \overset{(Q)}{\sigma}_{z_{nm}} \right\} + \sigma_{z_{n_{PART}}} \\
\tau_{rz_n} &= \sum_{m=1}^{K} \left\{ P_m \overset{(P)}{\tau}_{rz_{nm}} + Q_m \overset{(Q)}{\tau}_{rz_{nm}} \right\}
\end{aligned}
\tag{1-9}
$$

It can be seen that this problem is very complex. Consider, for example, the necessity of repeatedly evaluating eight difficult integral expressions, formulas (1-6). Note also the necessity of solving a stress matrix of $2 \cdot k$ simultaneous equations. Clearly, a computer solution is dictated. This solution is shown in Appendix A and contains several changes from that originally formulated in reference [1].

A trial and error approach was the only feasible method for checking this program. This entailed repeated

computer runs. The initial objective was to use this method to compare with the known results for a flat rotating disk. It was considered reasonable that before attempting to apply this method to the difficult problem of the unsymmetrical rotor, it should first be verified for the much simpler limiting case of the symmetrical disk. The choice of a symmetrical disk was particularly advantageous because symmetry simplified the problem of checking computer program results. Using the rotor of Fig. 2 as an example, the effects on the rotor periphery points of a load application at some point m=1 on the control contour, must be symmetrically related to the effects obtained by assuming load application at point m=14. This means that the coefficients, $P_m$ and $Q_m$, obtained from the solution of the stress matrix, equations (1-8), must be symmetrically related. Since $\sigma_r$ and $\sigma_\theta$ at point n=1, Fig. 2, must be equal to $\sigma_r$ and $\sigma_\theta$ at point n=14, it was determined that in the computer program results $P_1$ must equal $-P_{14}$ and $Q_1$ must equal $Q_{14}$.

The computer program, in its initial form, when utilized to solve the stresses in a symmetrical disk, at first gave stress results which were several orders of magnitude in error. There was no symmetry either among the coefficients generated from the solution of the stress matrix, equations (1-8), or in the solution of the integral equations, equations (1-6).

Two major improvements in the computer program, Appendix A, were used to produce the desired symmetry. The TEST value

of the integration program SIMCON, used to solve equations (1-6), was found to be unrealistic. This value was reduced from 0.1 to $0.1 \times 10^{-5}$. The second major change was in the method of introducing the angles $\lambda_n$. These are the angles which the rotor surface makes with the plane of rotation and were initially introduced in radians. It was found that this method introduced significant errors in calculating the sin and cos functions of $2\lambda$. The $\lambda$ input was changed to an input of fractions of $\pi$ and an accurate method of calculating $\pi$ was added to the program.

These two program changes resulted in producing the desired symmetry relationships to an accuracy which was believed acceptable. The magnitude of the calculated stresses was still considerably in error, but this was felt to be a function of the location of the imaginary control boundary.

It was believed that the imaginary boundary or control contour location was a critical factor in achieving the desired results. A location too close to the rotor surface, was expected to give an irregular stress distribution. A location too distant from the rotor surface was expected to cause inaccuracies associated with limitations in the number of significant figures available. It was believed that a generous range of boundary locations existed which would provide both a smooth stress distribution and the desired accuracy. Based on this presumption, an attempt to determine this optimum location of the control contour was

undertaken.

The shape of the imaginary contour most thoroughly investigated was as shown in Fig. 2. Although the effects of several other control contours were studied, this particular contour was selected for primary effort since all points on it are approximately the same distance from the rotor boundary. Major effort was directed towards the case of 14 equally spaced points of assumed load application along the control contour. Other numbers were also studied to some extent, but 14 was selected to keep computer run time within reasonable limits, (15 to 40 minutes). Satisfying the boundary conditions at 14 rotor surface points was believed to approximate sufficiently the exact boundary conditions.

Shown in Figs. 3 and 4 is the known solution, [2], for radial and tangential stresses in a symmetrical disk of uniform thickness. These stresses have been non-dimensionalized by dividing by the normalizing factor

$$\sigma_o = \frac{(3+\nu)}{8} \rho \omega^2 R^2$$

and have been plotted against relative radius (r/R). Also shown on these figures are similar plots of the stress data obtained by assuming various locations of the imaginary boundary. As shown, an imaginary boundary contour located at a distance of 14 inches from the rotor middle surface gave the best results for both the radial and tangential stresses. A one inch range of boundary locations between 13.5 to 14.5 inches gave fair results. This range was much

narrower than expected. The results for assumed boundary locations less than 9 inches and greater than 16 inches are not shown. These were extremely erroneous and had to be rejected.

In the above investigation, the rotor material properties, dimensions, and speed used were

Poisson's ratio = $\nu$ = .3333

Rotor density = $\rho$ = .00072 (lb.sec.$^2$/in.$^4$)

Maximum radius = R = 12 (inches)

Thickness = t = 2 (inches)

Speed = = 11,500 (rpm)

Using an imaginary boundary with spacing parameter D=14 inches, Fig. 2, and a rotor of maximum radius R=12 inches, computer runs were made with different values of the quantities $\nu$ , $\rho$ , and $\omega$. Theory indicates that variation of these quantities should have no effect on the accuracy of the results. The computer solution agreed with this theory, giving results of the same degree of accuracy.

The best results in Figs. 3 and 4 were obtained for a value of D/R=7/6. Maintaining this ratio, geometrically similar disks of differing absolute value of maximum radius R and thickness t were investigated. This non-dimensional ratio D/R was believed to be the principal scale factor. If the proper ratio were maintained, the stress solution for geometrically similar disks should be accurate. Again, the results of the computer solution justified this assumption. The accuracy of the results was

not significantly different from that previously obtained.

Since the computer formulation now gave essentially the correct results for flat disks, the next logical step was to study symmetrical disks of variable thickness. The special case of a disk of uniform stress was selected. [5]. For this type of rotor the stress is given by

$$\sigma = \sigma_r = \sigma_\theta = -\frac{\rho\omega^2 R^2}{2\ln\left(\frac{H}{h_0}\right)}$$

where

H = rotor thickness at r=R

$h_o$ = rotor thickness at r=0

Values of H, $h_o$, $\rho$, $\omega$, and R were selected to generate a rotor whose dimensions varied from those of the flat disk as shown below

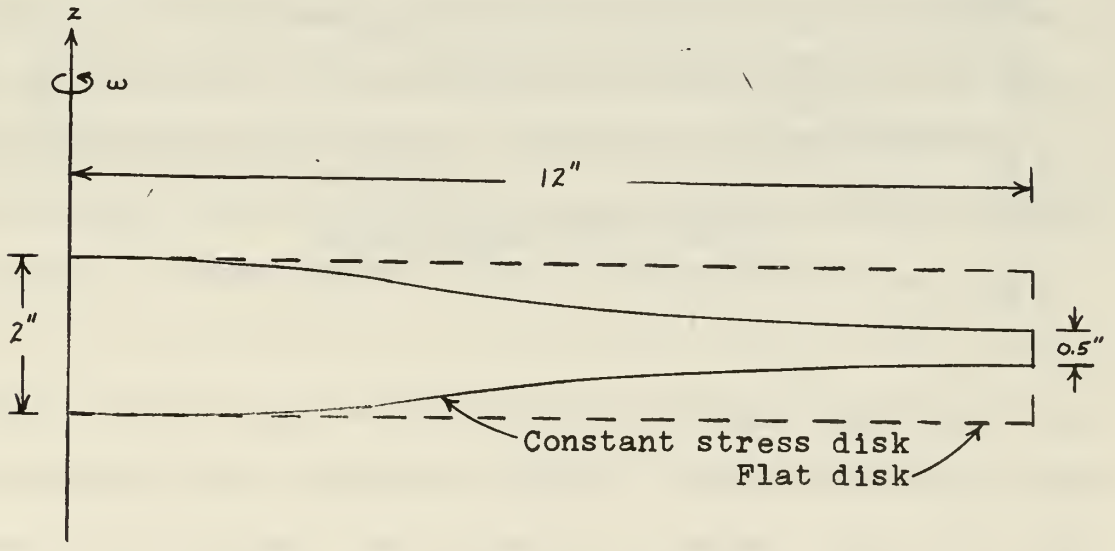


The thickness (h) at any point (r) was determined from

$$h = H e^{-\frac{\rho\omega^2 r^2}{2\sigma}}$$

The slope of the rotor contour at the selected points (r)

was determined from

$$\frac{dh}{dr} = -\frac{h\rho\omega^2 r}{\sigma}$$

These results were introduced into the computer program. The ratio D/R=7/6 was maintained. The computed stresses did not correlate with the known stress ($\sigma$). No constant stress of any magnitude was obtained. The generated stresses were in error up to an order of magnitude of ten.

As a further check of the solution, a coned rotor of constant thickness was introduced. The dimensions of this rotor varied from the flat disk as shown.

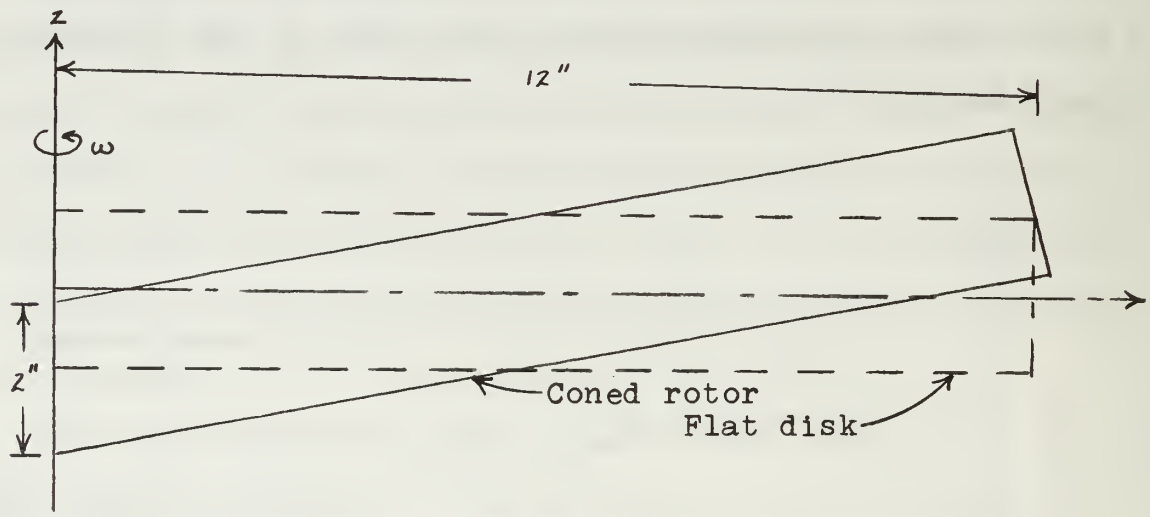


The theoretical solution for this rotor shape is given in Part III of this report. Again the results were unfavorable. Both radial and tangential stresses were completely erroneous. In both these cases it was noted that the results were extremely sensitive to very slight variation in the coordinates (r) and (z) which defined the rotor periphery points (n). That is, a change of only .01 inches in the value of the z

coordinate at one point could, for example, change all stresses by a factor of ten. Similar sensitivity to minor changes in the slope ($\gamma$) of the rotor contour was noted.

After many tests with both the constant stress shape and the coned rotor shape, no satisfactory results were obtained.

## CONCLUSIONS AND RECOMMENDATIONS

Application of the proposed solution to the limiting case of a flat symmetrical disk suggested that the theory was sound. However, for other rotor shapes, no acceptable results could be obtained. The extreme reaction of the computer solution to minor changes in rotor contour suggests that the solution as presently programmed is inherently unstable. The reason for this sensitivity is not known. It is believed to be associated with the solution of the stress matrix. In view of the obvious benefits to be obtained if this solution can be stabilized, further investigation of these difficulties is warranted.

## PART II: HOT SPIN TEST UNIT EVALUATION

### GENERAL DESCRIPTION

The hot spin test unit, designed and built for the aeronautical propulsion laboratories of the United States Naval Postgraduate School by the Baldwin-Lima-Hamilton Corporation, was accepted from the contractor on 22 November 1965. This unit is designed for testing various types of turbine and compressor rotors at both ambient and elevated temperatures. Both strain gage and thermocouple readings can be recorded during operation.

The test unit consists of four major components: The spin tank and drive assembly, the vacuum service unit, the heating system, and the control console.

The unit is designed to test rotors up to 50 inches in diameter with a maximum axial length of 24 inches. Maximum recording speed is 50,000 revolutions per minute. Maximum design rotor rim temperature is 1800 F.

The test unit can be driven by either of two sizes of air turbines. These are the Pelton turbine rated for speeds up to 30,000 rpm, or the Barbour-Stockwell turbine rated for speeds up to 50,000 rpm. The choice of drive turbine to be utilized is fixed by the size of the rotor to be tested.

The output from the strain gages or thermocouples which are mounted on the test rotor, passes through a slip ring assembly to reach the recorder. Two such assemblies are supplied with the test unit. The Superior Carbon slip

ring assembly has 36 rings available and the Lebow unit has 16 rings. The number of strain gages that can be used in each test depends on the slip ring assembly used, and on the method of wiring the bridge network. A common wire bridge system will allow the use of 36 strain gages using the Superior Carbon assembly or 16 gages using the Lebow assembly. However, since the test unit recorder has only 12 channels, use of more than 12 gages will require changing the wiring to the recorder during the test being conducted.

The output from the slip ring assembly is fed into a Minneapolis-Honeywell Electronik 15 multipoint recorder. The output from the thermocouples is recorded directly on a strip chart calibrated from 0 to 2000 F. The output from the strain gages is recorded as a strain signal in millivolts, printed on a strip chart calibrated from 0 to 10 millivolts. Printed data on the strip charts can be read with an accuracy of .01 millivolts and 1 degree F.

## EVALUATION PROCEDURES

Before conducting any tests on rotors of unknown stress distribution, it was deemed necessary to calibrate the recording system, and to test the slip ring assemblies for inherent errors and/or errors due to frictional heating. In conducting these tests, only the strain measuring system of the hot spin test unit was evaluated. Testing of the temperature recording capabilities remains for future investigation. All tests were conducted at ambient temperatures.

In testing the strain recording capabilities, two types of experimental runs were made. In the first of these, the slip ring devices and the strain recorder were evaluated with no test rotor installed in the unit. The second type runs had a test rotor installed.

An initial series of runs was made to determine if heating of the slip ring brushes would introduce errors. Both slip ring assemblies were tested. The Superior Carbon unit, which has intermittent brush contact and air cooling, was thought to be particularly susceptible to this type of error. The Lebow slip ring assembly, with continuous brush contact and freon cooling, was expected to be less subject to heating error.

In order to establish the presence of heating error, a pair of strain gages was applied to an external uniaxial aluminum test specimen. One of these gages was then wired so that its output would pass in one slip ring and out a second slip ring. The strain could then be read in millivolts on the multipoint recorder. The second gage on the test specimen was wired directly into the multipoint recorder and its strain also read in millivolts. Comparison of these readings was then used to estimate slip ring assembly losses.

The modulus of elasticity of the test specimen was found by the methods of Appendix B. When the specimen was loaded with a known weight, the induced strain could be calculated. A comparison of this known strain value with the two strain values printed by the recorder was used to detect any error

introduced by the recorder itself, and any error due to slip ring heating.

Both slip ring assemblies were tested in this manner, with readings taken at 1000 revolutions per minute intervals from 0 to 20,000 rpm.

After independently evaluating the slip ring assemblies and the recorder, it was next deemed necessary to install a test rotor in the spin unit and establish the ability to obtain accurate strain measurements at various speeds. A second series of runs was conducted for this purpose.

A test rotor, of which Fig. 5 is a simplified sketch, was designed and built to specifications in the Aeronautical Engineering Department machine shop. This test rotor was a 12 inch diameter flat disk of 0.5 inch thickness made from 2024 T4 aluminum plate. Fig. 17 in a folder attached to the back cover of this report, is a machinist's drawing of the test rotor. This simple shape was chosen since a theoretical solution was readily available. Several test specimens were tested in tension and torsion to establish accurate values of Young's Modulus (E), density ($\rho$), modulus of rigidity (G), and Poisson's ratio ($\nu$). A complete description of these tests can be found in Appendix B.

Ten SR-4, 350 ohm strain gages, five in the tangential direction and five in the radial direction, were placed on the test rotor at the locations shown in Fig. 5. For reasons of economy, these were not temperature compensating gages,

and no attempt at temperature compensation was made during these first tests.

The read-out in millivolts of the multipoint recorder is associated with the change in voltage across two legs of a Wheatstone bridge, caused by resistance change in the gage being strained. The strain gage is one leg of the bridge, and the other three legs consist of 350 ohm resistors which are wired into the circuit at the junction board of the control console. A diagram of the circuit is shown below.

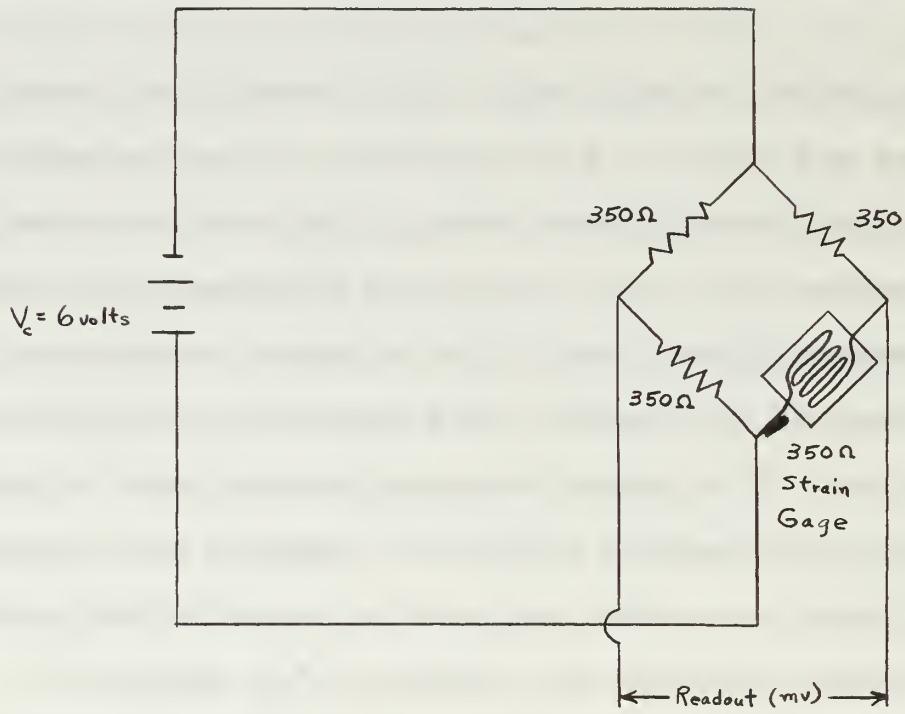


The millivolt read-out was then converted by the relationship [4]

$$\epsilon = \frac{(4000)\,\Delta V}{(G.F.)(V_c)} \qquad \left(\frac{\mu\ in.}{in.}\right) \tag{2-1}$$

where

$\Delta V$ = recorder reading (mv)

G.F. = gage factor

$V_c$ = impressed circuit voltage (volts)

These strains were then converted to stresses in the radial and tangential directions by the stress-strain relationships

$$\sigma_r = \frac{E}{(1-\nu^2)}(\epsilon_r + \nu\epsilon_\theta) \qquad (2\text{-}2)$$

$$\sigma_\theta = \frac{E}{(1-\nu^2)}(\epsilon_\theta + \nu\epsilon_r)$$

The test data was recorded at various speeds from 1000 to 20,000 revolutions per minute using both the Superior Carbon and the Lebow slip ring assemblies.

## RESULTS AND DISCUSSION

The first series of tests pertained to the evaluation of heating losses and inherent losses in the slip ring assemblies and recording equipment. A total of four evaluation runs were conducted, two for each slip ring assembly. Data from these runs established that the multipoint recorder gave very accurate readings ($\pm$ 1%) and that if the carrier voltage of the test circuit was maintained at six volts or below, heating effects in the slip ring assemblies were negligible.

The second series of tests pertained to the strain measuring capabilities of the hot spin test unit. Tests were conducted with both slip ring assemblies using the

rotor of Fig. 5.

Four runs were made with the Superior Carbon assembly installed. All ten strain gages, Fig. 5, were wired through the slip ring assembly. In addition, the external gages described in the previous section were included in the test runs for verification purposes. Gage number nine shorted out after assembly, but all other gages were active.

Unfortunately, none of these four runs involving the Superior Carbon assembly, yielded usable strain data. Although the gages themselves appeared to be in workable order and gave proper readings when used with the Lebow assembly, the data recorded was extremely erratic, and the recorded strains were not repeatable from one run to the next. However, the external gage which was wired through the slip ring assembly, gave acceptable results and did not vary during the four runs.

During these tests with the Superior Carbon device, a great amount of difficulty was encountered in joining the slip ring lead wires to the strain gage lead wires. The method of attachment provided by the manufacturer was unrealistic and impossible to accomplish. An alternate coupling was manufactured by the Aeronautical Engineering Department machine shop. Unfortunately, this coupling was designed so that the connection between the strain gage lead wires and the slip ring lead wires had to be accomplished at an appreciable distance from the spin axis. Furthermore, when the test unit is assembled, the inaccessi-

bility of the junction point required strain gage lead wires of excessive length. This surplus wiring had to be tied or taped to the rotor spindle. It was felt that this method of attachment allowed centrifugal strains to be induced in the lead wires near the junction point. These induced strains were believed to be of comparable magnitude to the strains within the gages themselves, and therefore this attachment proved completely unsatisfactory.

A series of three test runs were next made with the Lebow slip ring assembly, using the same rotor and strain gage arrangement as described above. However, gages 9 and 10 were eliminated due to the limited capacity of this unit.

These tests were considered successful. Table I contains a partial listing of the raw data recorded and the computed radial and tangential stresses that these data represent. Gage number two, which was at a radius of five inches, shorted out at the start of the testing. This reduced the usable data to points at radii of 1.5 inches and 3.25 inches.

In order to have a basis for comparison of the measured stresses, the two dimensional theoretical stresses for a disk with no hole at the center, [2] , were calculated from the following formulas.

$$\sigma_r = \frac{(3+\nu)}{8} \rho \omega^2 (R^2 - r^2) \qquad (2\text{-}3)$$

$$\sigma_\theta = \frac{(3+\nu)}{8} \rho \omega^2 R^2 - \frac{(1+3\nu)}{8} \rho \omega^2 r^2$$

It was believed that equations (2-3) give a good approximation of the test rotor stresses since the hole at the center of the test rotor is small, ($\frac{1}{4}$ inch diameter), and since the test rotor has compensating reinforcement near the center.

The test results are compared in the following manner. Figs. 6 and 7 are plots of radial and tangential stresses at two particular radii, against the square of centrifugal speed. The theoretical stresses at each radius (r) are plotted using equations (2-3) and appear as straight lines. The measured stresses are plotted as points for each centrifugal speed tested. The method of least squares from the theory of probability and statistics was used to analyze the measured data. The slope of the best straight line through the measured test points was found as shown in Appendix C. The dashed lines of Figs. 6 and 7 are these lines. The amount of data scatter was analyzed by determining the estimated standard deviation. This determination is shown in Appendix C. The overall estimated standard deviation of stress was found to be 159 psi. Using as a reference the maximum stress in a disk rotating at 17,500 rpm, the ratio of standard deviation to reference stress is 1.2%. Dividing the overall stress deviation by the modulus of elasticity gives a mean overall standard deviation of strain of 15 microinches per inch. This small deviation indicates that the strain values obtained from the test apparatus are excellent. In determining the slope of the best

straight line through the measured test points, it was assumed at the outset that this line passed through the origin. The small standard deviation of stress shows this to be a valid assumption. Furthermore, the fact that these lines do indeed pass through the origin confirms the findings of earlier test runs which showed that there was a negligible amount of constant error in the test apparatus.

Figs. 8 and 9 are non-dimensionalized plots of stress versus radius for the radial and tangential directions respectively. The system of coordinates shown was chosen since the stresses for all centrifugal speeds will plot as a single line. For a disk with no hole, the stress is greatest at the center. This stress was used as a normalizing factor. At the center of the disk

$$\sigma_o = \sigma_r = \sigma_\theta = \frac{(3+\nu)}{8} \rho \omega^2 R^2$$

Figs. 8 and 9 show clearly the relationship between theoretical and measured stresses in the rotor. The circled points on these figures are the slope of the measured lines of Figs. 6 and 7. These figures reveal an excellent correlation between measured and theoretical values at a radius of 3.25 inches. However, at a radius of 1.5 inches the measured radial stress was about 2.5 per cent greater than predicted and the measured tangential stress about 7 per cent less than predicted. These measurements were taken close to the reinforced center section of the rotor, Fig. 17, and it appears that the tangential stresses were somewhat relieved

in this area. At the same time, the radial stresses were somewhat augmented. These conditions represent a situation of over reinforcement of the center section of the disk. It is probable that removing some of the reinforcement would give better stress correlation at all radii.

It has been shown that the strain data obtained from the test unit was excellent. Any improvement in this data would most likely be realized by the use of temperature compensating strain gages. Minor factors which could have introduced errors include inherent strain gage accuracy ($\pm 2.5$ ohms), imprecise strain gage alignment in the principal directions, and centrifugal speed variations of the order of 300 rpm during data recording.

## CONCLUSIONS AND RECOMMENDATIONS

The hot spin unit of the Aeronautical Propulsion Laboratory is capable of accurately measuring strains in rotating specimens when the Lebow slip ring assembly is utilized. Using this configuration, the mean overall standard deviation of strain was 15 microinches per inch. Although reduction in data scatter may be slight, it is recommended that temperature compensating strain gages be used.

The measured stresses in a symmetrical disk determined from the hot spin unit were generally in good agreement with theoretical values. Differences in these values are primarily attributed to a test rotor which varied somewhat from

theoretical.

At present, it is not possible to measure strains using the Superior Carbon slip ring assembly. After evaluating the test runs made with this apparatus, it is concluded that the erratic behavior of the measured strains is most likely caused by the method of joining the strain gage lead wires to the slip ring assembly. It is therefore recommended that a connector be designed for the Superior Carbon slip ring assembly similar to the plug-in type connector used on the Lebow device. This plug-in method is considered the most convenient and economical means of connecting rotor and slip ring wiring.

Along with the above conclusions, the following recommendations are offered to future users of the hot spin test unit:

1. Use a well calibrated and accurate voltmeter to monitor the carrier voltage of the Wheatstone bridge, as this voltage is an important factor in reducing the millivolt read-out to a strain value. Maintaining the carrier voltage below six volts is necessary to prevent errors due to heating.

2. When installing a test rotor, the allowable runout at bottom of the lower arbor is .003 inches. It is nearly impossible to align the test rotor with the turbine shaft to these tolerances with the shaft mounted in the turbine. It is much easier to remove the turbine shaft, attach and align it with the test rotor, and then insert the two as a

single unit into the drive turbine.

3. When inserting the turbine shaft and rotor into the drive turbine, use a piece of thin walled hollow tubing to hold the excess lead wiring coming from the top of the turbine shaft. In this way you will not damage the bearings and magnetic seal of the drive turbine.

4. When balancing a test rotor using the Tinius-Olsen dynamic balancing machine belonging to the Mechanical Engineering Department, it is sufficient to balance to within ten of the smallest units of the finest setting of the balancing machine.

# PART III: CENTRIFUGAL STRESSES IN CONICAL ROTORS

## INTRODUCTION

In Part I of this report a method of obtaining centrifugal stresses in rotors of arbitrary and unsymmetrical cross section was attempted. On the presumption that this solution would prove satisfactory, it was felt that investigation of the special case of a conical rotor of constant thickness would be beneficial in validating this solution. A sample conical rotor was fabricated for this purpose. However, as explained, the general solution obtained in Part I proved unstable, and consequently an alternate method of analytically determining the stresses in a conical rotor was deemed necessary.

This section presents a method of determining the centrifugal elastic stresses in a coned rotor of constant thickness. From this solution the theoretical stresses in a ten degree coned rotor were determined. Comparative measured stresses for this specific case were obtained from the spin test facilities described in Part II of this report.

## ANALYSIS

### EXACT THEORETICAL SOLUTION FOR CENTRIFUGAL STRESSES IN A CONICAL ROTOR.

If a rotating disk is axisymmetric but has no plane of symmetry normal to the axis of rotation, the stresses at any radius vary over the thickness. Considering Fig. 10, it is evident that across some arbitrary section AB, the rotor material beyond AB will exert both a centrifugal force and a resultant bending moment about the center of AB. This bending moment can be of considerable magnitude.

The basic assumptions of this analysis are as follows. The material satisfies Hooke's Law. The stresses are linear across the thickness of the disk. Deformations are assumed to be small. The weight of the disk is neglected and the only forces acting upon it are those induced by rotation. Shear and axial stresses are negligibly small and linear elements parallel to the axis of rotation are assumed to remain linear.[1] The rotor is assumed homogeneous with no hole at the center. The effects of any material reinforcement near the center is neglected.

Fig. 11 is an element of this disk with the equilibrium expressed in terms of the distributed forces $T_r$ and $T_\theta$ and the distributed bending moments $M_r$ and $M_\theta$ computed

1. Hodge and Papa, [3], assumed linear elements parallel to the axis of rotation. This assumption was also used for the present analysis. The correctness of this assumption for rotors having large cone angles requires further investigation.

about the mean height $\bar{h}$. Considering the body force due to motion and considering equilibrium only in the radial direction leads to

$$\frac{d(rT_r)}{dr} - T_\theta + \rho\omega^2 r^2 h = 0$$
$$\frac{d(rM_r)}{dr} - M_\theta r T_r \frac{d\bar{h}}{dr} = 0 \qquad (3\text{-}1)$$

Considering a linear element which was initially parallel to the z axis, the displacement of the centroid, [3], may be written as

$$u_r(r,z) = u(r) - [z - \bar{h}(r)]\,\phi(r) \qquad (3\text{-}2)$$

where u(r) is the radial displacement and $\phi(r)$ is the angle through which it is rotated. The strain displacement relationships are

$$\epsilon_r = \frac{\partial u_r}{\partial r} = \frac{du}{dr}(z-\bar{h})\frac{d\phi}{dr} + \phi\frac{d\bar{h}}{dr}$$
$$\epsilon_\theta = \frac{u_r}{r} = \frac{u}{r} - (z-\bar{h})\frac{\phi}{r} \qquad (3\text{-}3)$$

The applicable stress-strain equations are

$$\sigma_r = \frac{E}{(1-\nu^2)}(\epsilon_r + \nu\epsilon_\theta)$$
$$\sigma_\theta = \frac{E}{(1-\nu^2)}(\epsilon_\theta + \nu\epsilon_r) \qquad (3\text{-}4)$$

Equations (3-1), (3-2), (3-3), and (3-4) may be reduced to the following set of equations

$$\frac{d}{dr}\left(\frac{T_\theta}{h}\right) - \nu \frac{d}{dr}\left(\frac{T_r}{h}\right) - \frac{(1+\nu)}{r h}\left(T_r - T_\theta\right) + \frac{12\bar{h}'}{h^3}\left(M_\theta - \nu M_r\right) = 0$$

$$\frac{d}{dr}\left(\frac{M_\theta}{h^3}\right) - \nu \frac{d}{dr}\left(\frac{M_r}{h^3}\right) - \frac{(1+\nu)}{r h^3}\left(M_r - M_\theta\right) = 0 \qquad (3\text{-}5)$$

It is desired to express this problem in terms of stress functions. A pair of stress functions which satisfy the equilibrium equations (3-1) identically is defined by

$$\begin{aligned} T_r &= \frac{\Psi}{r} \\ T_\theta &= \Psi' + \rho\omega^2 r^2 h \\ M_r &= \frac{\chi}{r} \\ M_\theta &= \chi' - \Psi\bar{h}' \end{aligned} \qquad (3\text{-}6)$$

Substitution of equations (3-6) into equations (3-5) yields [3] the following two second order differential equations for the stress functions.

$$\begin{aligned} &\Psi'' + \left(1 - \frac{r h'}{h}\right)\frac{\Psi'}{r} - \left[1 - \nu\frac{r h'}{h} + 12\left(\frac{r\bar{h}'}{h}\right)^2\right]\frac{\Psi}{r^2} \\ &\quad + \frac{12}{h}\frac{r\bar{h}'}{h}\left(\frac{\chi'}{r} - \nu\frac{\chi}{r^2}\right) + (3+\nu)\rho\omega^2 r h = 0 \\ &\chi'' + \left(1 - 3\frac{r h'}{h}\right)\frac{\chi'}{r} - \left(1 - 3\nu\frac{r h'}{h}\right)\frac{\chi}{r^2} \\ &\quad - r\bar{h}'\left[\frac{\Psi'}{r} + \left(1 + \nu - 3r\frac{h'}{h} + r\frac{\bar{h}''}{\bar{h}'}\right)\frac{\Psi}{r^2}\right] = 0 \end{aligned} \qquad (3\text{-}7)$$

Fig. 10 represents a coned rotor of arbitrary cone angle $\alpha$ rotating about the z axis at angular speed $\omega$. The

mean height $\bar{h}$ and the thickness h and their derivatives with respect to the z axis are given by

$$\begin{aligned} \bar{h} &= r \tan\alpha \\ \bar{h}' &= \tan\alpha \\ \bar{h}'' &= 0 \\ h &= \text{constant} \\ h' &= h'' = 0 \end{aligned} \tag{3-8}$$

Substitution of equations (3-8) into equations (3-7) yields two second order differential equations

$$\begin{aligned} \psi'' + \frac{\psi'}{r} - \left[C_1 + \frac{1}{r^2}\right]\psi + C_2\left[\chi' - \nu\frac{\chi}{r}\right] + C_3 r = 0 \\ \chi'' + \frac{\chi'}{r} - \frac{\chi}{r^2} + C_4\psi' - C_5\frac{\psi}{r} = 0 \end{aligned} \tag{3-9}$$

where, for convenience we adopt temporarily the notation

$$\begin{aligned} C_1 &= 12\left(\frac{\tan\alpha}{h}\right)^2 \\ C_2 &= 12\frac{\tan\alpha}{h^2} \\ C_3 &= (3+\nu)\rho\omega^2 h \\ C_4 &= \tan\alpha \\ C_5 &= (1+\nu)\tan\alpha \end{aligned}$$

It was assumed that the solutions, $\psi$ and $\chi$, to equations (3-9) were in the form of power functions of r. Since no direct particular and complementary solutions could be

determined, the following power series was utilized.

$$\Psi = A_0 + A_1 r + \frac{A_2 r^2}{2!} + \frac{A_3 r^3}{3!} + \frac{A_4 r^4}{4!} + \cdots + \frac{A_n r^n}{n!} + \cdots$$
$$\chi = B_0 + B_1 r + \frac{B_2 r^2}{2!} + \frac{B_3 r^3}{3!} + \frac{B_4 r^4}{4!} + \cdots + \frac{B_n r^n}{n!} + \cdots \qquad (3\text{-}10)$$

The substitution of equations (3-10) into equations (3-9) yields two equations containing the unknown coefficients $A_0$, $A_1$, $A_2$, ---- and $B_0$, $B_1$, $B_2$, -----. These equations have a non-trivial solution only if the sum of the coefficients multiplying each power of r is identically zero. This approach leads to the following set of equations to be solved

$$-A_0 = 0$$
$$\left[A_1 - A_1 - \nu C_2 B_0\right] = 0$$
$$A_2\left[1+1-\frac{1}{2!}\right] + C_2 B_1 (1-\nu) = 0$$
$$A_3\left[1+\frac{1}{2!}-\frac{1}{3!}\right] + C_2 B_2\left(1-\frac{\nu}{2!}\right) - C_1 A_1 + C_3 = 0$$
$$A_4\left[\frac{1}{2!}+\frac{1}{3!}-\frac{1}{4!}\right] + C_2 B_3\left(\frac{1}{2!}-\frac{\nu}{3!}\right) - \frac{C_1 A_2}{2!} = 0 \qquad (3\text{-}11)$$

— — — — — — — — — — —

$$A_n\left[\frac{1}{(n-2)!}+\frac{1}{(n-1)!}-\frac{1}{n!}\right] + C_2 B_{n-1}\left[\frac{1}{(n-2)!}-\frac{\nu}{(n-1)!}\right] - \frac{C_1 A_{n-2}}{(n-2)!} = 0$$
$$-B_0 = 0$$
$$\left[B_1 - B_1 - C_5 A_0\right] = 0$$
$$B_2\left[1+1-\frac{1}{2!}\right] - A_1\left[C_4 + C_5\right] = 0$$

$$B_3\left[1+\frac{1}{2!}-\frac{1}{3!}\right]-A_2\left[C_4+\frac{C_5}{2!}\right]=0$$

$$B_4\left[\frac{1}{2!}+\frac{1}{3!}-\frac{1}{4!}\right]-A_3\left[\frac{C_4}{2!}+\frac{C_5}{3!}\right]=0 \qquad (3\text{-}11)$$

— — — — — — — — —

$$B_n\left[\frac{1}{(n-2)!}+\frac{1}{(n-1)!}-\frac{1}{n!}\right]-A_{n-1}\left[\frac{C_4}{(n-2)!}+\frac{C_5}{(n-1)!}\right]=0$$

From equations (3-11) $A_0$ and $B_0$ are identically zero. These equations further reveal $A_1$ and $B_1$ to be arbitrary constants. The $n^{th}$ term equations reveal an interdependence of the even numbered A constants and odd numbered B constants and conversely the even numbered B constants are related to the odd numbered A constants. After algebraic manipulation of equations (3-11), expressions for generalized constants $A_n$ and $B_n$ are

$$A_n=-A_{n-2}\,\lambda^2\frac{1}{(n-2)(n+1)}$$

$$B_n=-B_{n-2}\,\lambda^2\frac{(n+\nu)}{(n-2)(n+1)(n-2+\nu)} \qquad (3\text{-}12)$$

where

$$\lambda^2=12\left(\frac{\tan\alpha}{h}\right)^2(1-\nu^2)$$

Further expansion shows that equations (3-12) can be written in the form

$$A_n=\frac{1}{\lambda}\lambda^n a_n$$

$$B_n=\frac{1}{\lambda^2}\lambda^n b_n \qquad (3\text{-}13)$$

where

$$a_n = -a_{n-2}\frac{1}{(n-2)(n+1)}$$
$$b_n = -b_{n-2}\frac{(n+\nu)}{(n-2)(n+1)(n-2+\nu)} \qquad (3\text{-}14)$$

Using equation (3-13), the $n^{th}$ terms of equations (3-10) become

$$\frac{A_n}{n!}\rho^n = \frac{a_n}{\lambda n!}(\lambda r)^n$$
$$\frac{B_n}{n!}\rho^n = \frac{b_n}{\lambda^2 n!}(\lambda r)^n \qquad (3\text{-}15)$$

where the quantity ($\lambda$r) is non-dimensional.

Several of the relationships of equations (3-11) are dependent upon centrifugal speed. Equations (3-14) reveal the association that exists between all a and b constants. From these observations it is concluded that the general solution, equations (3-10), consists of a particular solution dependent upon centrifugal speed and two complementary solutions dependent upon the arbitrary constants $a_1$ and $b_1$.

The first of the complementary solutions is obtained by setting the arbitrary constant $a_1$ equal to 1.0, with $b_1$ and $\omega$ identically zero. Functions obtained are

$$\psi_1(\lambda r) = \sum_{n=1,3,5,\cdots}^{\infty}\frac{a_n}{n!}(\lambda r)^n \qquad (3\text{-}16a)$$
$$\chi_1(\lambda r) = \sum_{n=2,4,6,\cdots}^{\infty}\frac{b_n}{n!}(\lambda r)^n$$

where

$$a_1 = 1.0$$

$$b_2 = \tfrac{2}{3}(2+\nu)\tan\alpha$$

and where $a_n$ and $b_n$ are obtained from equations (3-14).

In a like manner, setting $b_1$ equal to 1.0 with $a_1$ and $\omega$ identically zero gives the second complementary solution as

$$\psi_2(\lambda_R) = \sum_{n=2,4,6,\cdots}^{\infty} \frac{a_n}{n!}(\lambda_R)^n$$
$$\chi_2(\lambda_R) = \sum_{n=1,3,5,\cdots}^{\infty} \frac{b_n}{n!}(\lambda_R)^n \qquad (3\text{-}16b)$$

where

$$b_1 = 1.0$$
$$a_2 = -\tfrac{3}{2}\ \frac{12\tan\alpha}{h^2}(1-\nu)$$

with $a_n$ and $b_n$ obtained from equations (3-14).

Functions for the particular solution obtained by setting $a_1$ and $b_1$ equal to zero are given by

$$\psi_\omega(\lambda_R) = \sum_{n=1,3,5,\cdots}^{\infty} \frac{a_n}{n!}(\lambda_R)^n$$
$$\chi_\omega(\lambda_R) = \sum_{n=2,4,6,\cdots}^{\infty} \frac{b_n}{n!}(\lambda_R)^n \qquad (3\text{-}16c)$$

where

$$a_1 = b_1 = 1.0$$
$$a_3 = -\tfrac{3}{4}$$
$$b_4 = -\tan\alpha\left[\tfrac{3}{5} + \tfrac{1}{5}(1+\nu)\right]$$

As before, $a_n$ and $b_n$ are obtained from equations (3-14).

Utilizing the above functions, the solution as originally formulated, equation (3-10), can be restated in equivalent form as

$$\Psi(\lambda_n) = \frac{(3+\nu)\rho\omega^2 h}{\lambda^3}\left[P\Psi_1(\lambda_n) + Q\Psi_2(\lambda_n) + \Psi_\omega(\lambda_n)\right]$$
$$\chi(\lambda_n) = \frac{(3+\nu)\rho\omega^2 h}{\lambda^4}\left[P\chi_1(\lambda_n) + Q\chi_2(\lambda_n) + \chi_\omega(\lambda_n)\right] \qquad (3\text{-}17)$$

Examination of the functions $\Psi_1$, $\Psi_2$, $\Psi_\omega$, $\chi_1$, $\chi_2$, and $\chi_\omega$ reveals that the terms in these functions alternate in sign, and all series converge rapidly.

Solution (3-17) consists of two equations having two unknowns, P and Q. Utilizing two boundary conditions for the specific problem under consideration will lead to a determination of these unknowns. Values of P and Q specify the stress functions $\Psi$ and $\chi$ and the corresponding stress distribution throughout the rotor.

For the case of a rotor with no external loads, the boundary conditions of zero stress in the radial direction and zero radial bending moment at maximum radius must be satisfied. This requires that

$$\Psi(\lambda R) = 0$$
$$\chi(\lambda R) = 0 \qquad (3\text{-}18)$$

where

$$R = r_{MAX.}$$

Substitution of these boundary conditions in equation (3-10) yields the following equations for P and Q.

$$P = \frac{\Psi_2 \chi_\omega - \chi_2 \Psi_\omega}{\Psi_1 \chi_2 - \Psi_2 \chi_1} \qquad (3\text{-}19)$$

$$Q = \frac{\chi_1 \Psi_\omega - \Psi_1 \chi_\omega}{\Psi_1 \chi_2 - \Psi_2 \chi_1}$$

where all functions are evaluated at r=R.

With these amplitudes determined, equations (3-17) will lead to values of $\Psi$ and $\chi$ for any desired radius r.

Radial and tangential stresses in the rotor are comprised of direct and bending stresses. [3] . These components are defined by

$$\begin{aligned} \sigma_{r_d} &= \frac{T_r}{h} \\ \sigma_{r_b} &= \frac{6 M_r}{h^2} \\ \sigma_{\theta_d} &= \frac{T_\theta}{h} \\ \sigma_{\theta_b} &= \frac{6 M_\theta}{h^2} \end{aligned} \qquad (3\text{-}20)$$

Substitution of equations (3-6) and (3-17) into equations (3-20), and non-dimensionalizing using a normalizing factor of $\sigma_0 = \frac{(3+\nu)}{8} \rho \omega^2 R^2$ leads to

$$\frac{\sigma_{r_d}}{\sigma_0} = \frac{8}{(\lambda R)^2} \left[ \frac{P \Psi_1(\lambda r) + Q \Psi_2(\lambda r) + \Psi_\omega(\lambda r)}{(\lambda r)} \right] \qquad (3\text{-}21)$$

$$\frac{\sigma_{r_b}}{\sigma_0} = \frac{48}{(\lambda R)^2 (\lambda h)} \left[ \frac{P \chi_1(\lambda r) + Q \chi_2(\lambda r) + \chi_\omega(\lambda r)}{(\lambda r)} \right]$$

$$\frac{\sigma_{\theta_d}}{\sigma_o} = \frac{8}{(\lambda R)^2}\left[P\psi_1'(\lambda r) + Q\psi_3'(\lambda r) + \psi_\omega'(\lambda r)\right] + \frac{8}{(3+\nu)}\left(\frac{\pi}{R}\right)^2$$

$$\frac{\sigma_{\theta_b}}{\sigma_o} = \frac{48}{(\lambda R)^2(\lambda h)}\left[P\chi_1'(\lambda r) + Q\chi_3'(\lambda r) + \chi_\omega'(\lambda r)\right] \qquad (3\text{-}21)$$

$$+ \frac{48\tan\alpha}{(\lambda R)^2(\lambda h)}\left[P\psi_1(\lambda r) + Q\psi_3(\lambda r) + \psi_\omega(\lambda r)\right]$$

In equations (3-6) the functions $\psi'$ and $\chi'$ are derivatives with respect to r. Note that the new functions, $\psi_1'$, $\psi_3'$, $\psi_\omega'$, $\chi_1'$, $\chi_3'$, and $\chi_\omega'$ are derivatives with respect to the dimensionless variable ($\lambda r$). Therefore, differentiation of equations (3-17) leads to

$$\psi' = \frac{d\psi}{dr} = \lambda\frac{d\psi}{d(\lambda r)} = \frac{(3+\nu)\rho\omega^2 h}{\lambda^2}\left[P\psi_1'(\lambda r) + Q\psi_3'(\lambda r) + \psi_\omega'(\lambda r)\right]$$

$$\chi' = \frac{d\chi}{dr} = \lambda\frac{d\chi}{d(\lambda r)} = \frac{(3+\nu)\rho\omega^2 h}{\lambda^3}\left[P\chi_1'(\lambda r) + Q\chi_3'(\lambda r) + \chi_\omega'(\lambda r)\right]$$

The new functions $\psi_1'$, $\psi_3'$, $\psi_\omega'$, $\chi_1'$, $\chi_3'$, and $\chi_\omega'$ become

$$\psi_1' = \frac{d\psi_1}{d(\lambda r)} = \sum_{n=1,3,5,\cdots}^{\infty}\frac{a_n}{(n-1)!}(\lambda r)^{n-1}$$

$$\psi_3' = \frac{d\psi_3}{d(\lambda r)} = \sum_{n=3,4,6,\cdots}^{\infty}\frac{a_n}{(n-1)!}(\lambda r)^{n-1}$$

$$\psi_\omega' = \frac{d\psi_\omega}{d(\lambda r)} = \sum_{n=1,3,5,\cdots}^{\infty}\frac{a_n}{(n-1)!}(\lambda r)^{n-1}$$

$$\chi_1' = \frac{d\chi_1}{d(\lambda r)} = \sum_{n=3,4,6,\cdots}^{\infty}\frac{b_n}{(n-1)!}(\lambda r)^{n-1}$$

$$\chi_3' = \frac{d\chi_3}{d(\lambda r)} = \sum_{n=1,3,5,\cdots}^{\infty}\frac{b_n}{(n-1)!}(\lambda r)^{n-1}$$

$$\chi_\omega' = \frac{d\chi_\omega}{d(\lambda r)} = \sum_{n=3,4,6,\cdots}^{\infty}\frac{b_n}{(n-1)!}(\lambda r)^{n-1}$$

with all constants $a_1$ through $a_n$ and $b_1$ through $b_n$ defined as before.

Using the assumption that the stresses are linear across the thickness of the disk, the stresses throughout the disk are completely determined by the stresses on the convex and concave faces. In the radial and tangential directions, these are designated $\sigma_{r_1}$ and $\sigma_{\theta_1}$ for the convex face, and $\sigma_{r_2}$ and $\sigma_{\theta_2}$ for the concave face. These non-dimensionalized surface stresses are given by

$$\begin{aligned}
\frac{\sigma_{r_1}}{\sigma_0} &= \frac{\sigma_{r_d}}{\sigma_0} + \frac{\sigma_{r_b}}{\sigma_0} \\
\frac{\sigma_{\theta_1}}{\sigma_0} &= \frac{\sigma_{\theta_d}}{\sigma_0} + \frac{\sigma_{\theta_b}}{\sigma_0} \\
\frac{\sigma_{r_2}}{\sigma_0} &= \frac{\sigma_{r_d}}{\sigma_0} - \frac{\sigma_{r_b}}{\sigma_0} \\
\frac{\sigma_{\theta_2}}{\sigma_0} &= \frac{\sigma_{\theta_d}}{\sigma_0} - \frac{\sigma_{\theta_b}}{\sigma_0}
\end{aligned} \qquad (3\text{-}22)$$

Substitution of equations (3-21) into equations (3-22) uniquely determines the radial and tangential surface stresses at any point on the rotor.

The foregoing solution is readily adapted to computer methods as shown in Appendix D. An expansion of this solution to include plots of the non-dimensionalized functions of the parameter ($\lambda r$) will render unnecessary the use of computer methods. This expansion is explained in the results and discussion section of this analysis.

CENTRIFUGAL STRESSES IN A TEN DEGREE CONED ROTOR.

As a validation of the previously discussed theoretical solution for the centrifugal stresses in a conical rotor, an investigation was conducted to determine the surface stresses of a particular case. The rotor chosen for this investigation was a coned rotor of constant thickness and a ten degree cone angle.

The test rotor was fabricated at the United States Naval Postgraduate School. It was made of 2024-T4 aluminum and the material properties were determined in the manner described in Appendix B. Pertinent material properties were found to be

$$\rho = .000258 \ \frac{lb.\,sec.^2}{in.^4}$$

$$\nu = .335$$

Fig. 12 is a sketch of the rotor used in this investigation. As shown, it had the following basic dimensions.

cone angle $= \alpha = 10$ degrees

thickness $= h = .5$ inches

radius $= r_{max} = 6$ inches

Strain gages (SR-4, 350 ohm) were attached at the locations shown in Fig. 12. The rotor was dynamically balanced and then installed in the spin test facility of the United States Naval Postgraduate School. The induced strains were found in accordance with the methods described in Part II of this report. The range of centrifugal speeds investigated was from 0 to 15,000 revolutions per minute.

The values of recorded strains were converted to radial

and tangential stresses in accordance with the procedures described in Part II of this report. Figs. 13 and 14 contain plots of the measured radial and tangential surface stresses versus the square of centrifugal speed at various radial distances on both the convex and concave surfaces. Figs. 15 and 16 contain plots of these same stresses non-dimensionalized, using a normalizing factor of $\frac{(3+\nu)}{8} \rho \omega^2 R^2$ for stress. This is plotted versus non-dimensionalized radius (r/R). The normalizing factor $\frac{(3+\nu)}{8} \rho \omega^2 R^2$ represents the maximum radial and tangential stresses in a symmetrical rotating disk. This factor was chosen to illustrate conveniently the stress levels.

Utilizing the previously discussed theoretical solution for the stresses in any coned rotor, an approximate solution for the stresses in this particular case was determined. This solution was approximate to the extent that a truncated six term series was used to represent each of the stress functions $\Psi$ and $\chi$ .

Appendix D is the computer program used for this specific problem. While its format is not readily recognizable as the exact solution presented, it is functionally the same except that it utilizes the two six term approximations mentioned. In its present form, this program computes the radial and tangential stresses on both the convex and concave rotor faces for radius increments of 0.25 inches. These stresses are listed for centrifugal speeds from 0 to 15,000 revolutions per minute in 1000 revolution per minute

increments.

Stress data from the computer solution is plotted on Figs. 13 through 16.

## RESULTS AND DISCUSSION

The exact theoretical solution described in Part III will accurately determine the stresses in any conical rotor of constant thickness. For disks without a central hole, the present solution may be readily extended to include arbitrary loading at the outer rim. For disks with a central hole it will be necessary to redefine the power series, equations (3-10), to include negative exponents. The method of solution will be similar to that presented, with the exception that the defining stress functions, equations (3-17), will consist of four complementary solutions and four arbitrary constants. These arbitrary constants will be determined by two boundary conditions at the rotor rim and two at the hole.

Equations (3-17) in the form presented are dimensional. These stress functions may be non-dimensionalized in the following manner.

$$\Psi^* = \frac{\lambda^3}{(3+\nu)\rho\omega^2 h}\,\Psi(\lambda_R) = P\Psi_1 + Q\Psi_2 + \Psi_\omega$$

$$\chi^* = \frac{\lambda^4}{(3+\nu)\rho\omega^2 h}\,\chi(\lambda_R) = P\chi_1 + Q\chi_2 + \chi_\omega$$

Since P and Q, from equations (3-19), are determined by the parameter ($\lambda$ R), it is enlightening to rewrite these

dimensionless stress functions in the form

$$\Psi^* = P(\lambda R)\,\Psi_1(\lambda r) + Q(\lambda R)\,\Psi_2(\lambda r) + \Psi_\omega(\lambda r)$$

$$\chi^* = P(\lambda R)\,\chi_1(\lambda r) + Q(\lambda R)\,\chi_2(\lambda r) + \chi_\omega(\lambda r)$$

This reveals that the stress functions for this problem are characterized by the single parameter $(\lambda R)$. This parameter is defined as

$$\lambda R = \sqrt{12(1-\nu^2)}\ t \tan\alpha \frac{R}{h}$$

Values of this parameter will define the distributed forces and the distributed bending moments, equations (3-6), in a conical rotor. It is noted that the final stresses are additionally dependent upon the parameters $(\tan\alpha)$ and $(1-\nu^2)$.

The argument of the 12 non-dimensionalized functions which appear in equations (3-21) is $(\lambda r)$. These functions can easily be tabulated and drawn over a range of values of $(\lambda r)$. Once this is done, a computer solution for this problem is unnecessary. For a specific problem being considered, $(\lambda R)$ is known. By entering the curves and tabulations with this value of $(\lambda R)$, P and Q are determined using equations (3-19). Reentering these curves with any selected value of $(\lambda r)$ and utilizing equations (3-21) will immediately lead to the direct and bending stresses at the corresponding rotor point.

The assumption of linear elements parallel to the axis of rotation may invalidate this general solution for rotors of large cone angles. This matter is unresolved and requires further investigation..

The utilization of the general solution to predict the centrifugal stresses in a ten degree coned rotor gave generally satisfactory results. Since all series rapidly converge, the use of six term approximations gave results nearly indistinguishable from the exact solution.

It was expected that all stresses would be linear with the square of centrifugal speed. Figs. 13 and 14 show this to be the case. The amount of measured data scatter reflected on these figures is of the same order of magnitude as that reflected in Part II of this report. Any improvement in these data would most likely be accomplished by the use of temperature compensating strain gages.

Figs. 15 and 16 contain the theoretical and comparative measured stresses obtained for this specific rotor. In general, the discrepancies between these values are somewhat greater than those observed in the symmetrical disk. It appears that the radial stresses at r=1.5 inches were somewhat augmented and the tangential stresses somewhat relieved. These deviations are again attributed to the differences between the test rotor and the theoretical rotor. The measured data again represents a situation of over reinforcement near the center section of the disk.

Figs. 15 and 16 additionally show the variation of radial and tangential stresses across the thickness of the disk versus relative radius. Comparison of these curves with similar curves for a symmetrical disk, Figs. 8 and 9, illustrate the following points.

In a symmetrical disk, stresses across the thickness of the disk are virtually constant. For a coned rotor there is obviously a large stress variation across the thickness. At relative radius locations less than .55, an element located on one rotor face is <u>in compression in both the radial and tangential directions!</u> An element located directly across the rotor on the opposite face is in tension in both directions.

In a symmetrical disk the radial and tangential stresses at the center, r=0, are equal. These stresses are also the maximum stresses developed and are of magnitude

$$\sigma_0 = \sigma_r|_{r=0} = \sigma_\theta|_{r=0} = \frac{(3+\nu)}{8} \rho \omega^2 R^2$$

For the specific conical disk considered, the stresses at the center are again equal. It is significant that these are not the maximum stresses generated within the rotor. The maximum middle surface radial stress occurs at a relative radius of approximately 0.6, and the maximum middle surface tangential stress occurs nearly at maximum radius. At the center of the conical disk, the magnitude of the middle surface stress is much less than in a symmetrical rotor, and this surface is actually in compression! At r=0, these stresses are

$$\sigma_r|_{r=0} = \sigma_\theta|_{r=0} = -.128 \frac{(3+\nu)}{8} \rho \omega^2 R^2$$

The largest stresses generated within the conical rotor are the compressive radial stress of the convex face at r=0, and the tensile tangential stress of the concave face at r=R.

## CONCLUSIONS AND RECOMMENDATIONS

The exact solution described in this section of the report will predict the stresses in any conical rotor of constant thickness. The parameter of importance in defining non-dimensional stress functions is ($\lambda R$). The detailed stresses are additionally dependent upon the parameters ($\tan \alpha$) and ($1-\nu^2$). It is recommended that systematic calculations be conducted assuming various values of ($\lambda R$), to determine the effects of this parameter on the rotor stress distribution.

It is recommended that the stress functions $\Psi_1$, $\Psi_2$, $\Psi_\omega$, $\chi_1$, $\chi_2$, and $\chi_\omega$, and their derivatives, be tabulated and plotted against ($\lambda r$). This will permit determining the stresses in any conical rotor of constant thickness without the necessity of using a computer.

The assumption of linear elements parallel to the axis of rotation requires further investigation to determine its validity for rotors of large cone angles.

For the specific rotor tested, the stresses of the middle surface were found to be generally less than in a symmetrical disk. The stresses on the faces however, were considerably larger than in a symmetrical disk. Stresses across the thickness of the disk were found to vary considerably, at some radial locations changing from compression on one face to tension on the other.

The measured stresses, as determined from the hot spin

unit of the United States Naval Postgraduate School, were generally in good agreement with theoretical values. The differences in these values are primarily attributed to an experimental rotor which varied somewhat from theoretical. A small amount of data scatter is attributed to strain gages which were not temperature compensated.

# BIBLIOGRAPHY


1. Johnson, R. A. Centrifugal Stresses in Rotors of Arbitrary Cross Section. United States Naval Postgraduate School, 1965.

2. Timoshenko, S. and Goodier, J. N. Theory of Elasticity. McGraw-Hill, 1951.

3. Hodge, P. G. Jr. and Papa, J. Rotating Disks with No Plane of Symmetry. The Franklin Institute, 1957.

4. Perry, C. C. and Lissner, H. R. The Strain Gage Primer. McGraw-Hill, 1962.

5. Prescott, J. Applied Elasticity. Longmans, Green, and Company, 1924.

ACKNOWLEDGMENT

The generous assistance and encouragement of Professor T. H. Gawain of the United States Naval Postgraduate School is gratefully acknowledged.

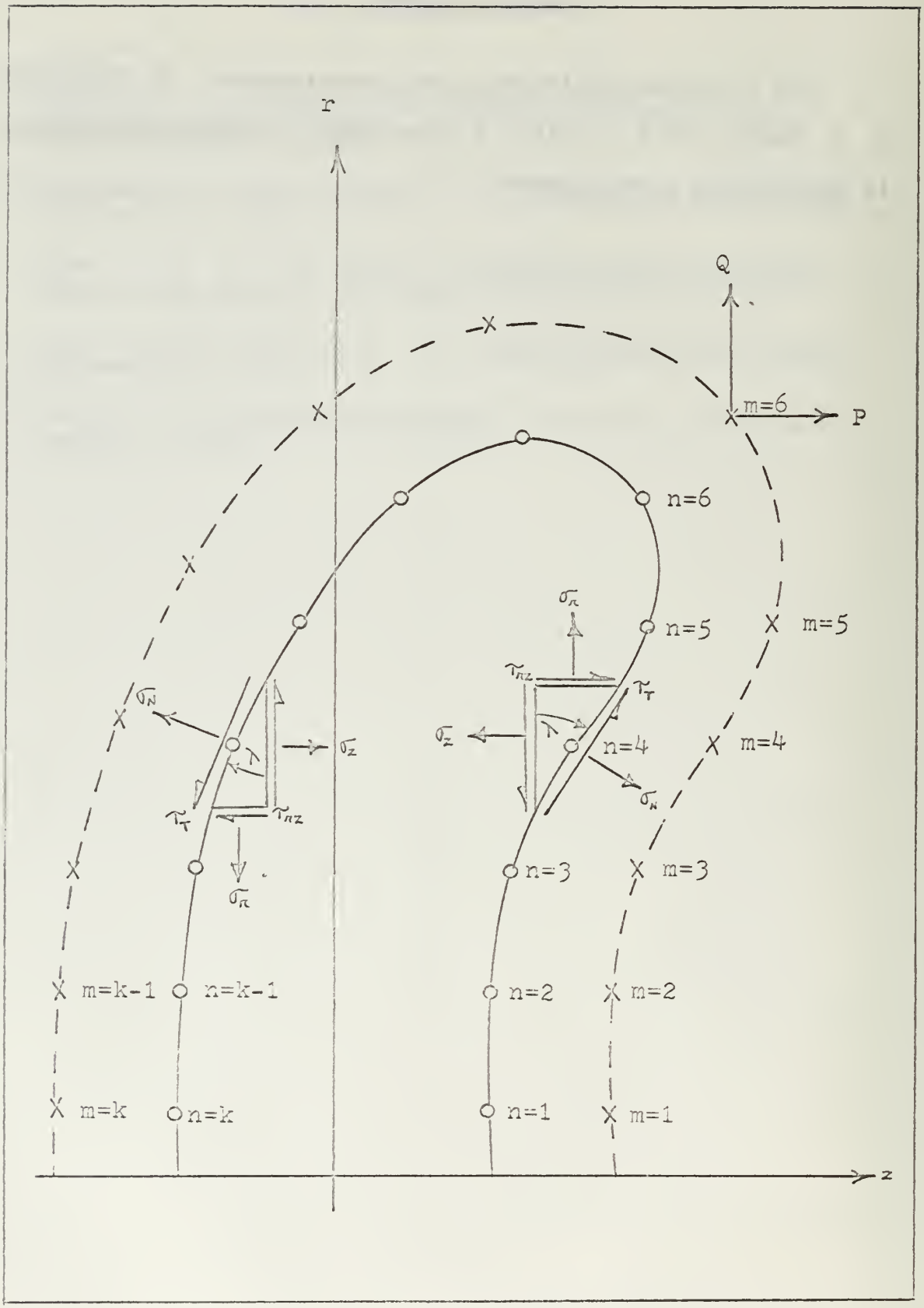


Fig. 1. Arbitrary rotor cross section with imaginary boundary

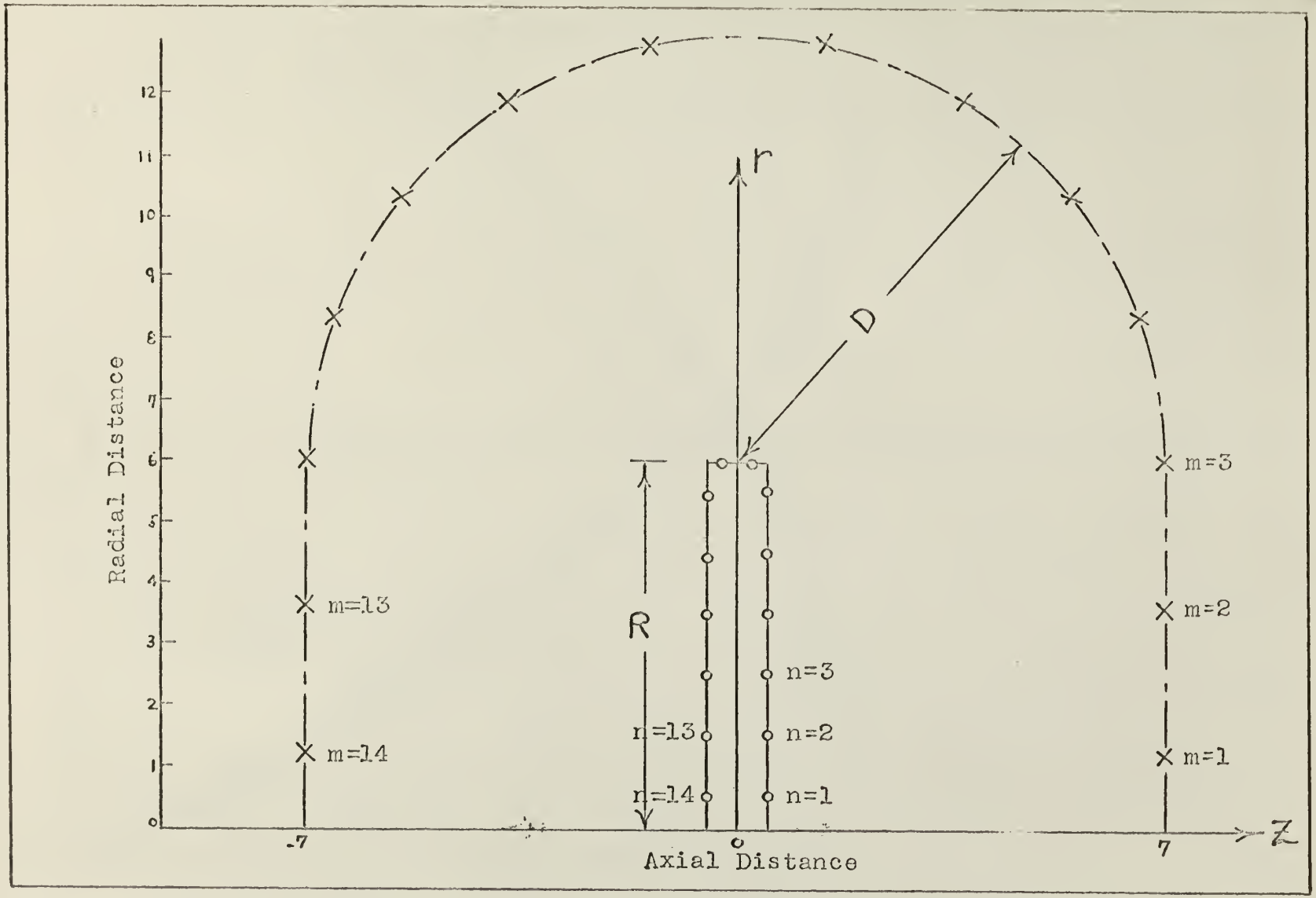


Fig. 2. Example Rotor Cross Section and Assumed Imaginary Boundary

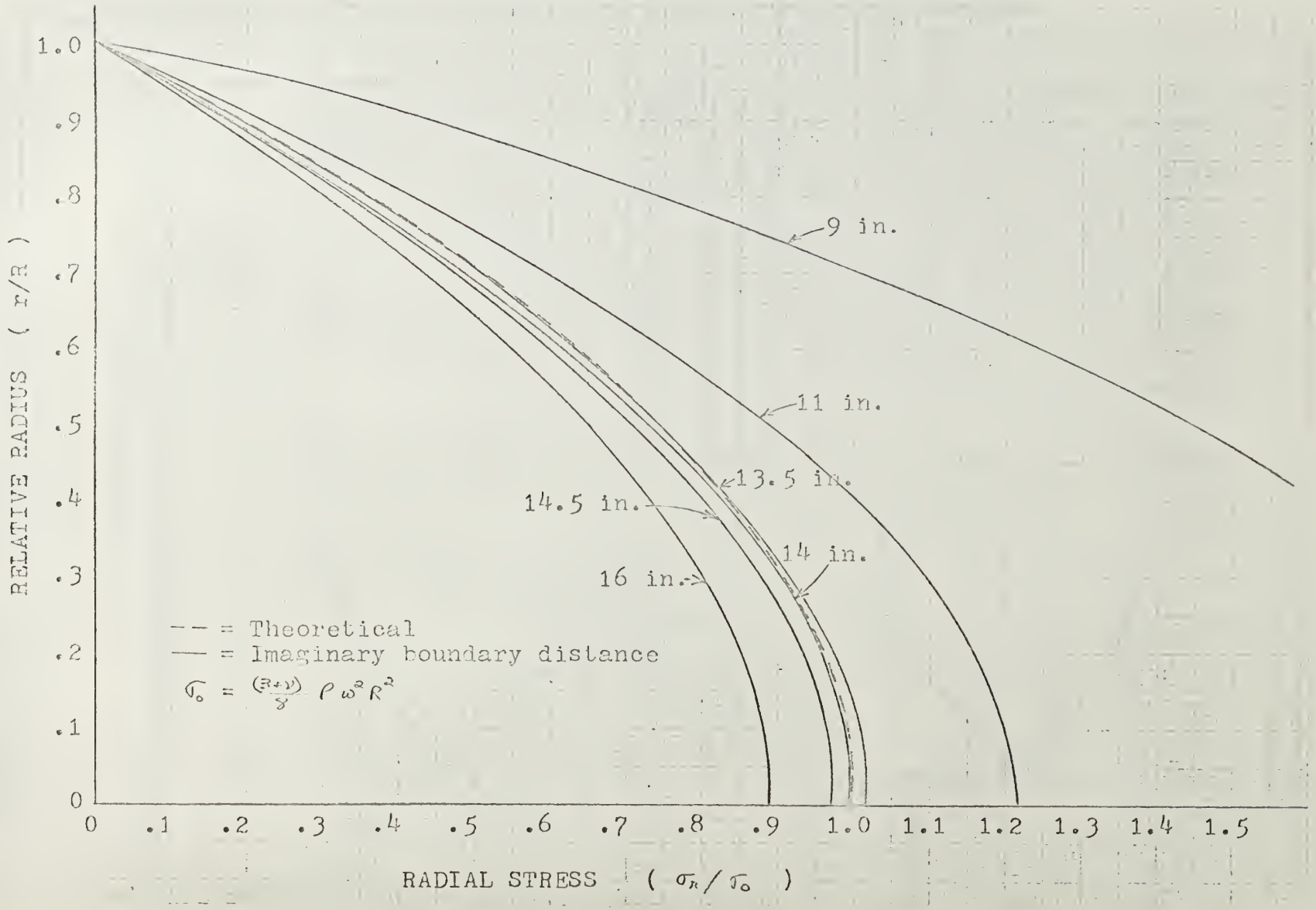


Fig. 3. Computer Results for Radial Stresses in a Flat Disk

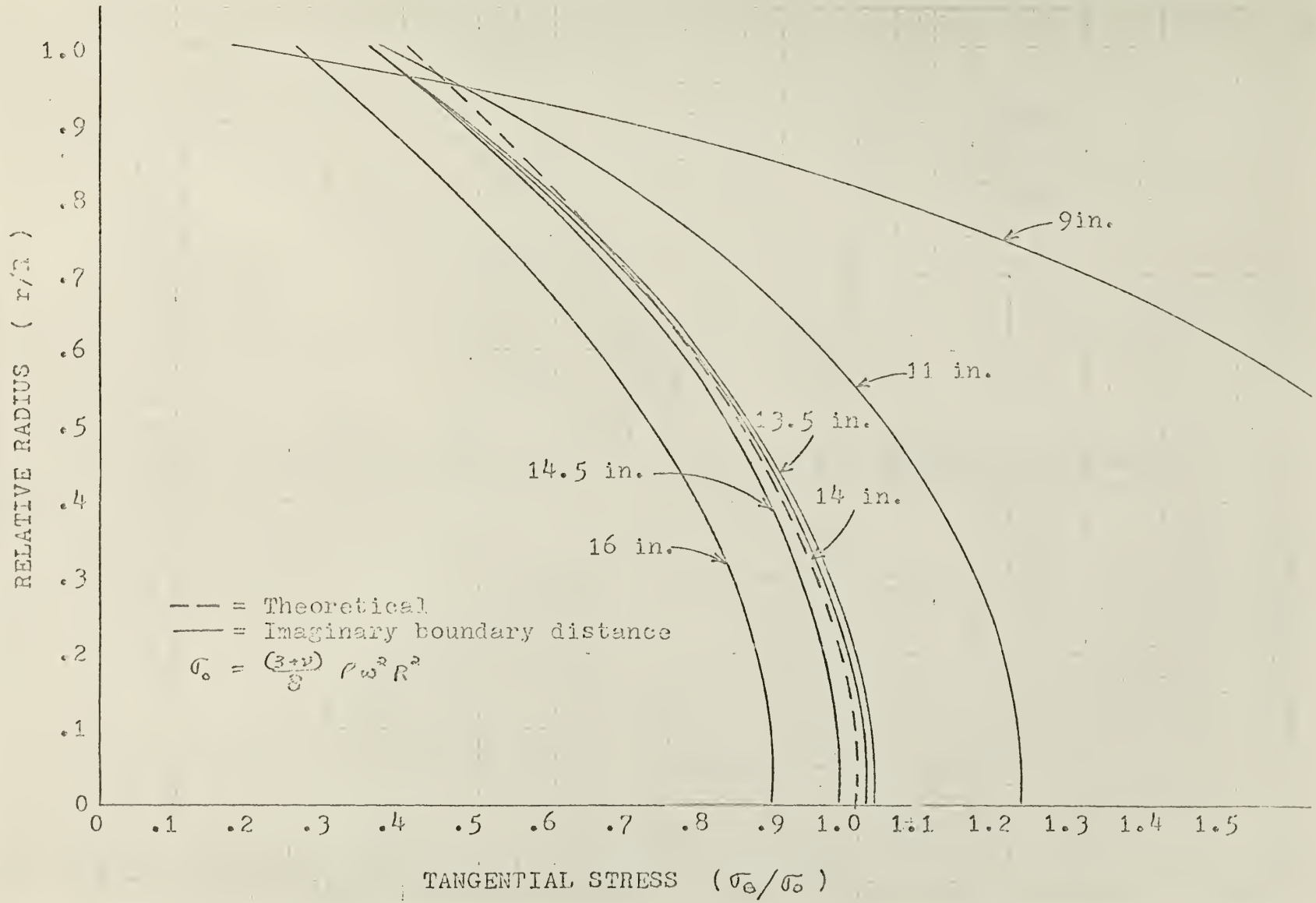


Fig. 4. Computer Results for Tangential Stresses in a Flat Disk

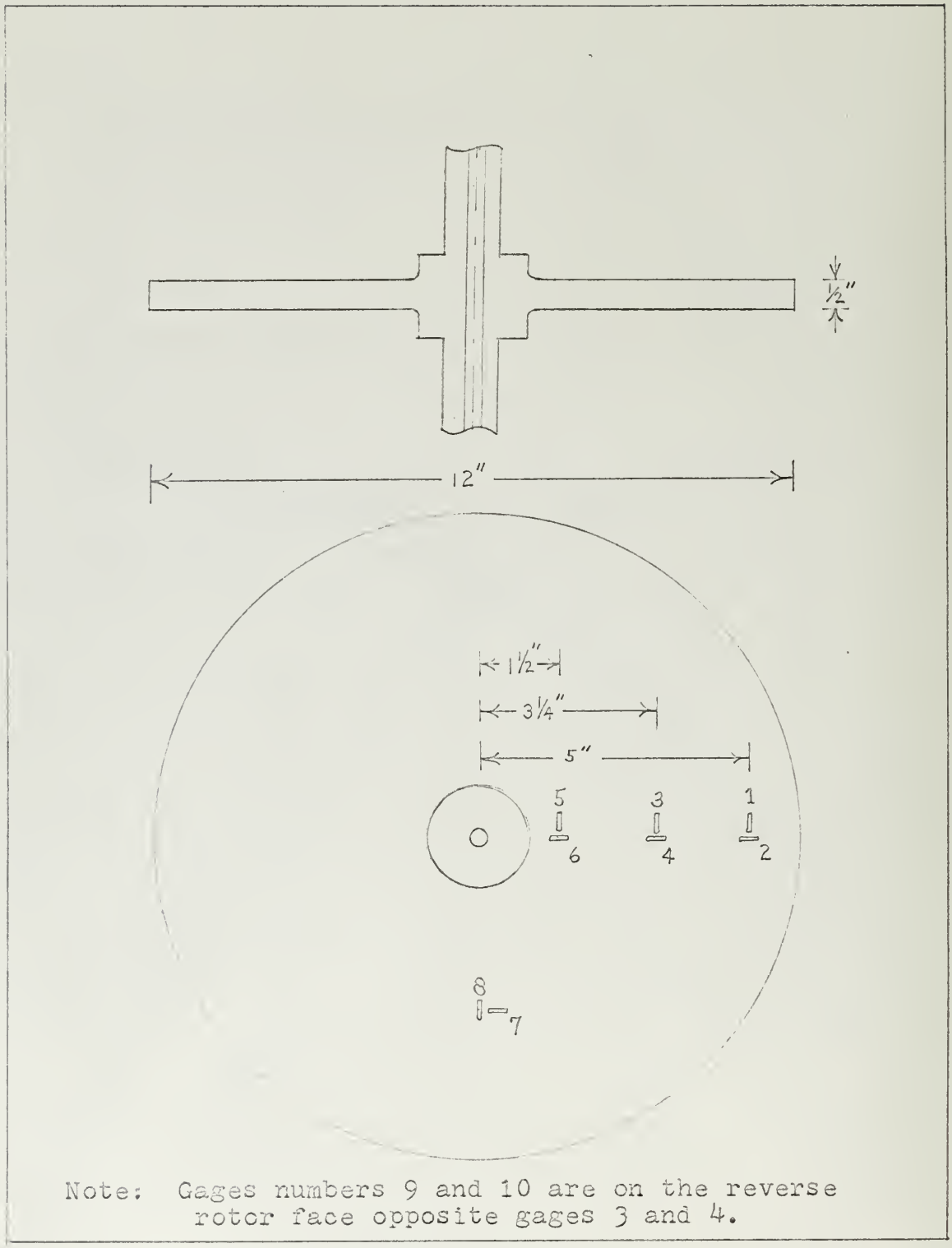


Note: Gages numbers 9 and 10 are on the reverse rotor face opposite gages 3 and 4.

Fig. 5. Symmetrical Disk Test Rotor and Strain Gage Placement

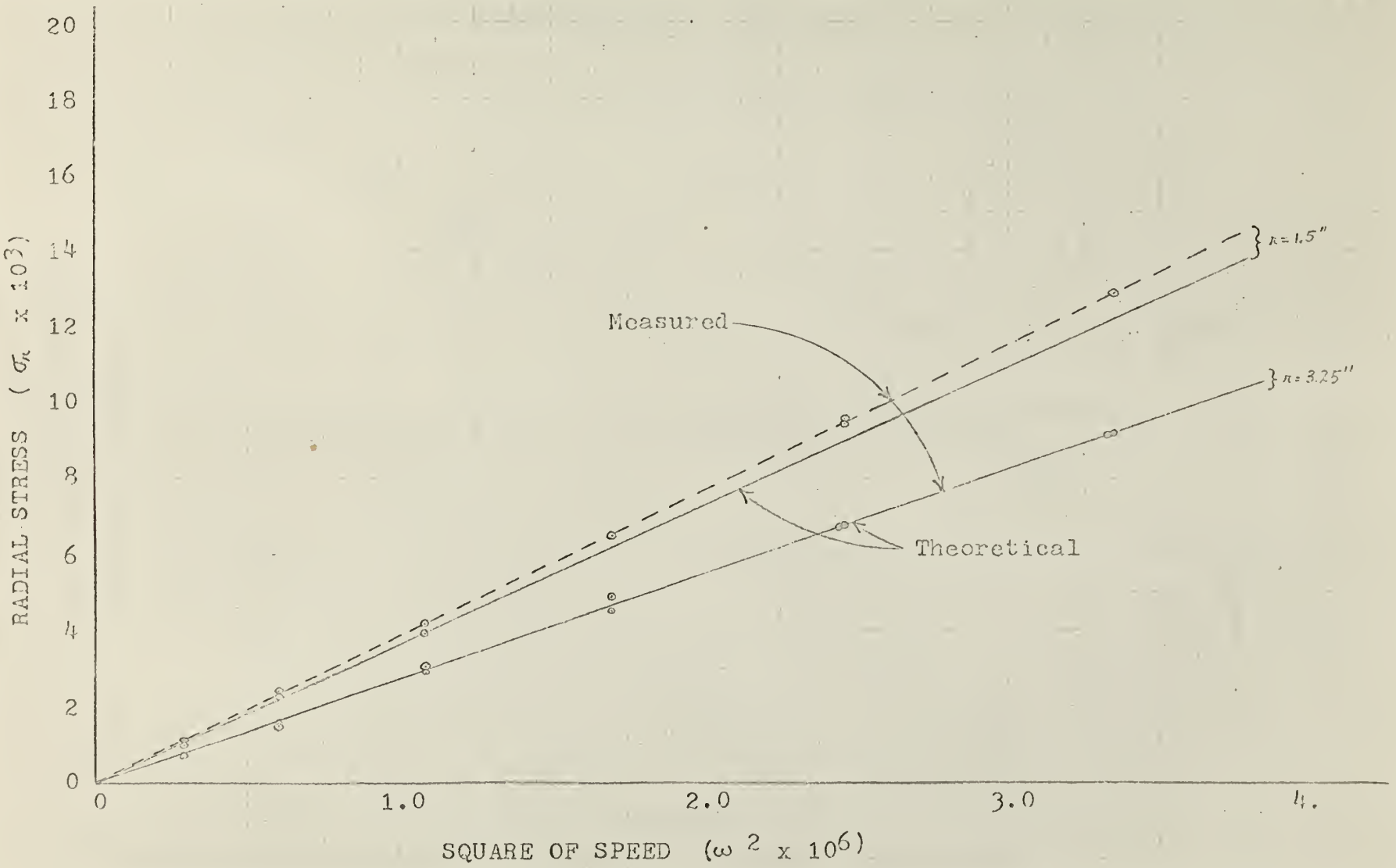


Fig. 6. Radial Stress in a Symmetrical Disk at Selected Radii

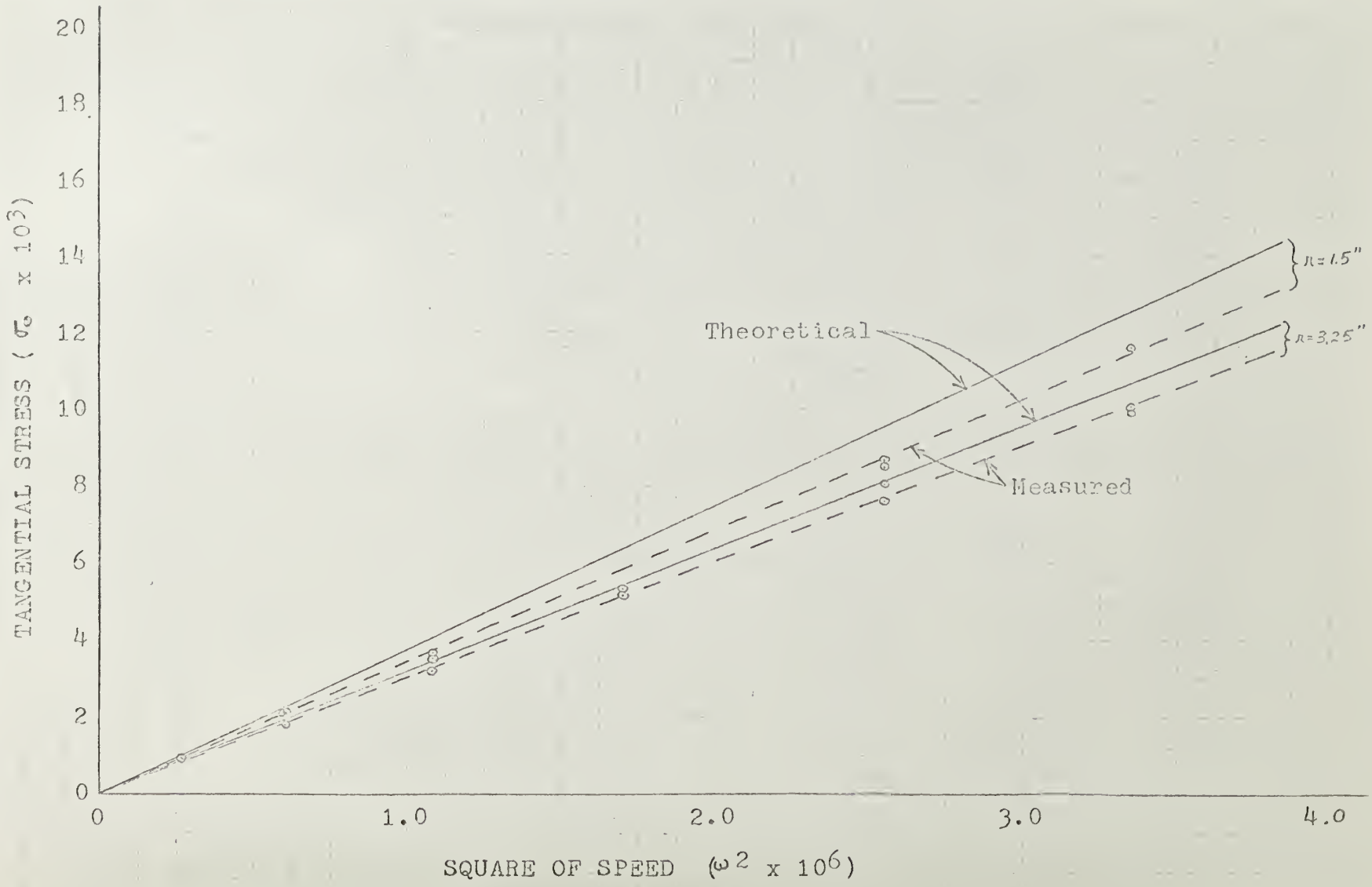


Fig. 7. Tangential Stress in a Symmetrical Disk at Selected Radii

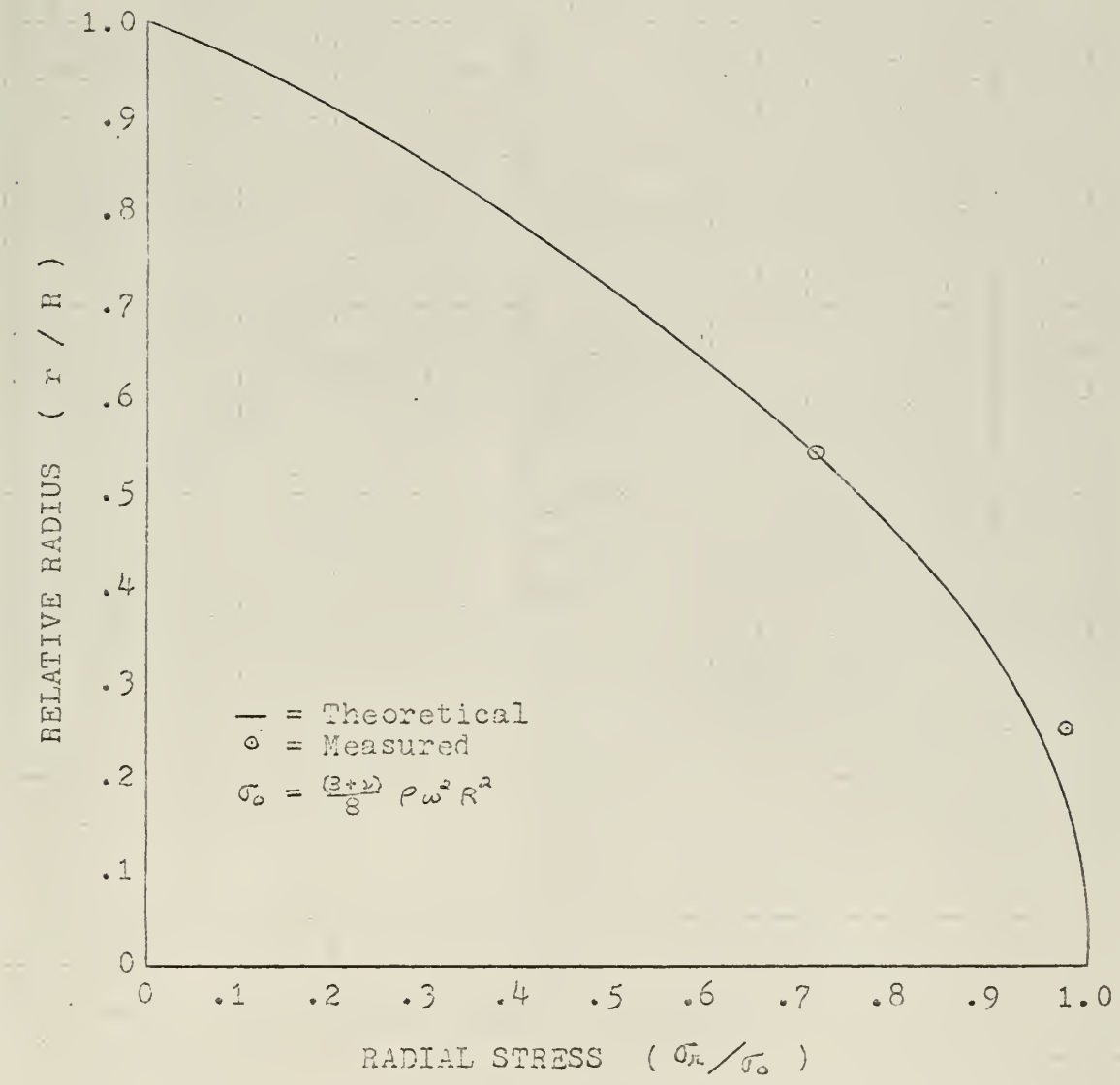


Fig. 8 . Radial Stress in Symmetrical Disk

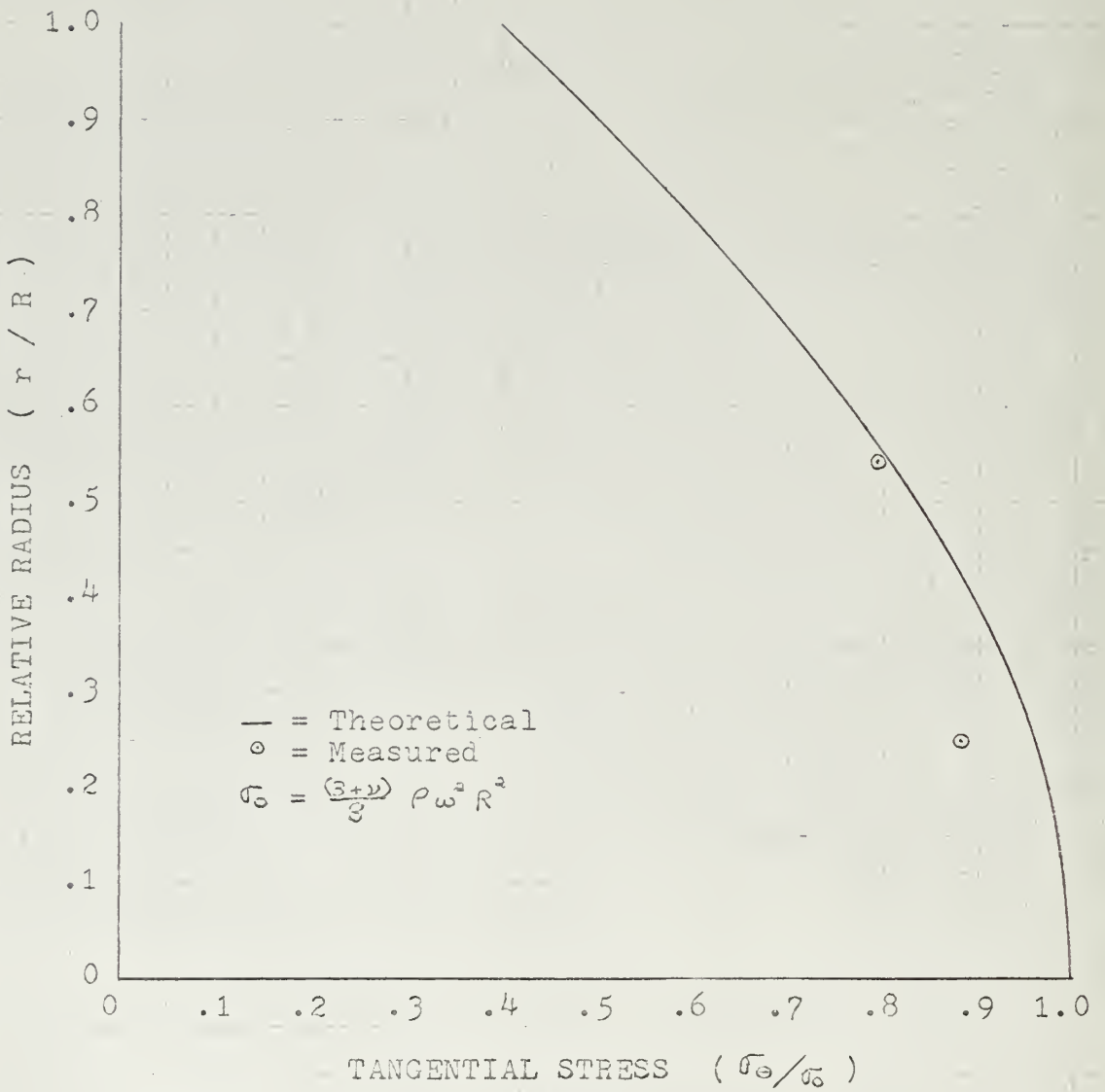


Fig. 9 . Tangential Stress in Symmetrical Disk

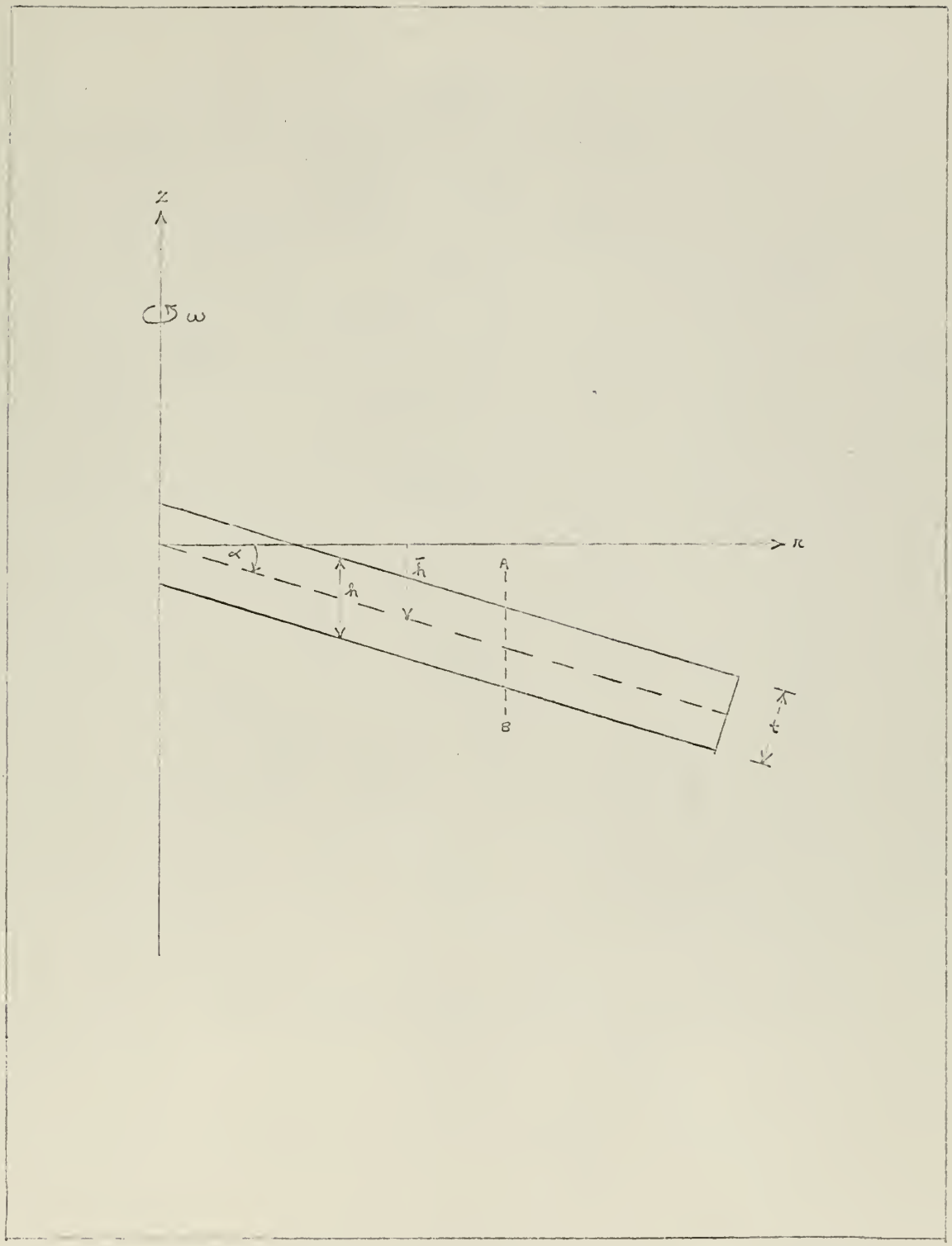


Fig. 10. Example Coned Rotor Cross Section

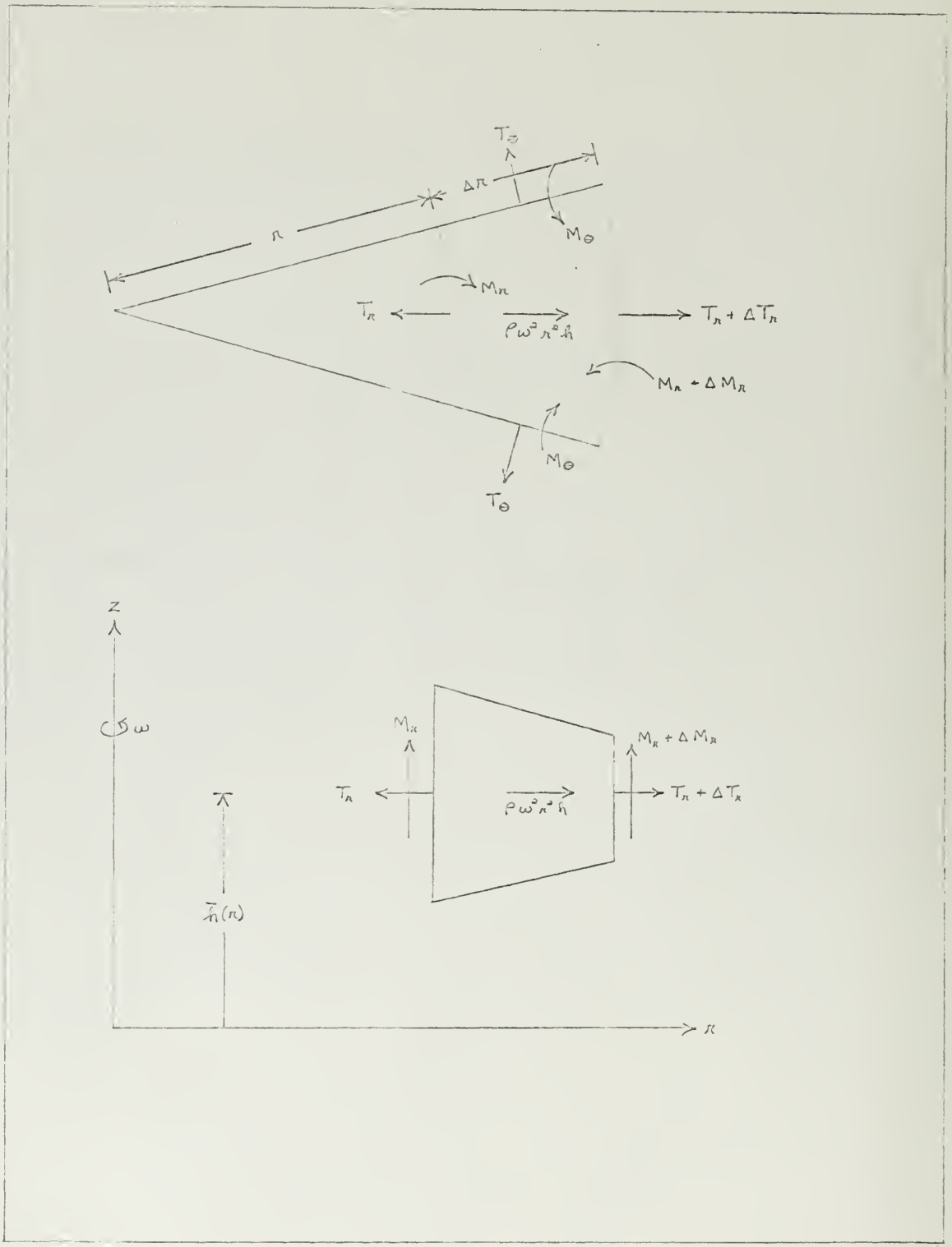


Fig. 11. Equilibrium of an Element in a Conical Rotor

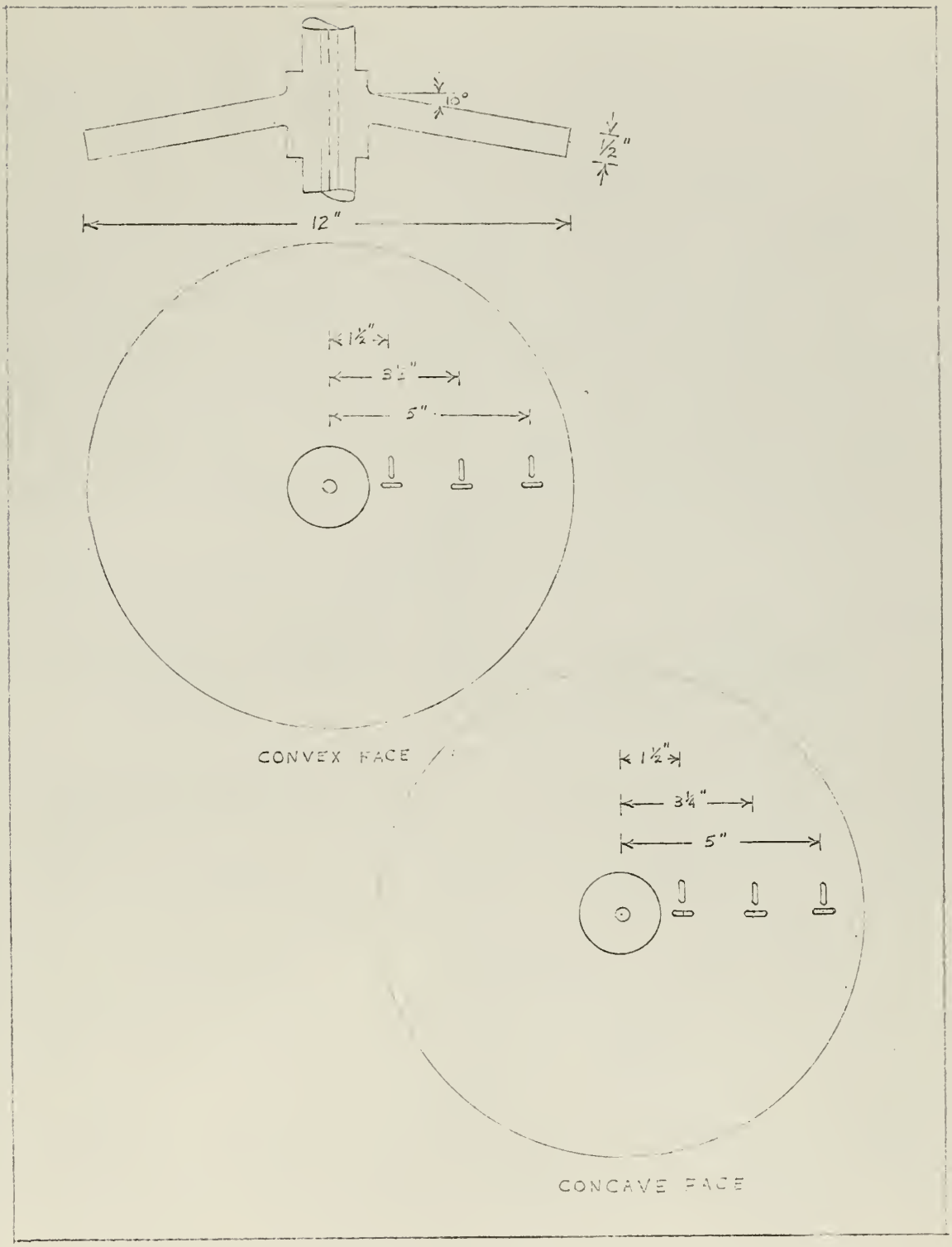


Fig. 12. Conical Test Rotor and Strain Gage Placement

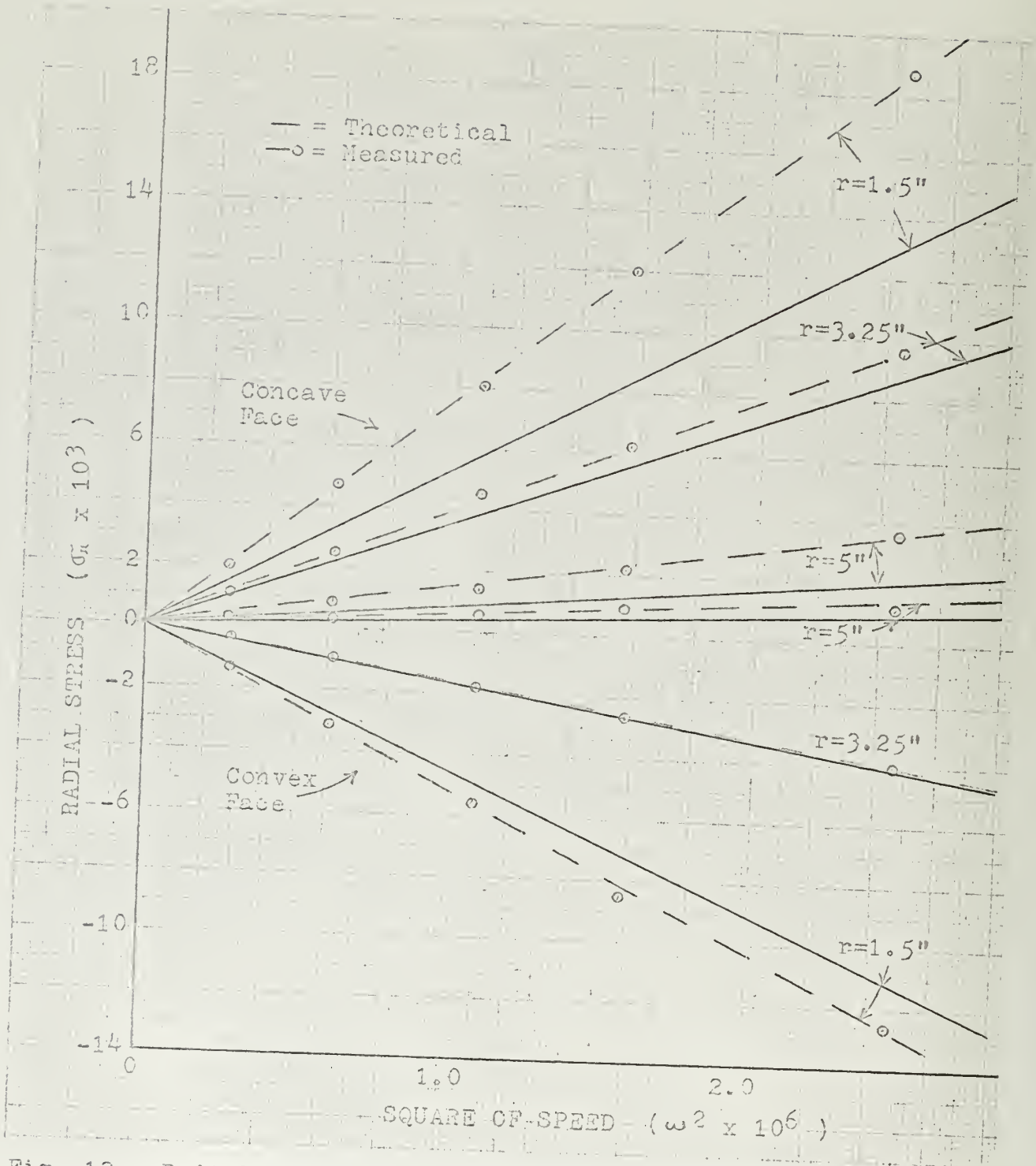


Fig. 13. Radial Stress in a Conical Disk at Selected Radii

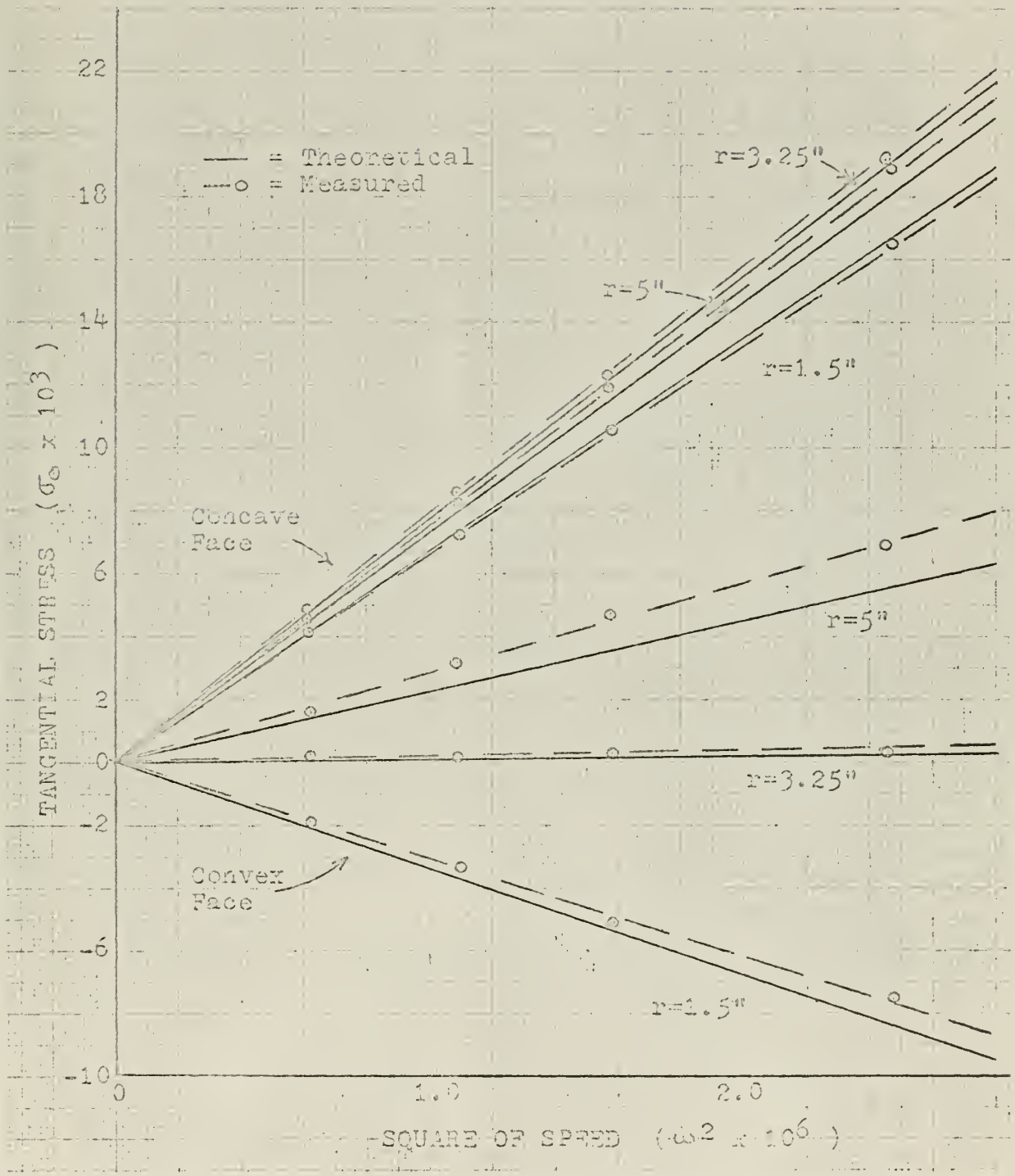


Fig. 14. Tangential Stress in a Conical Disk at Selected Radii

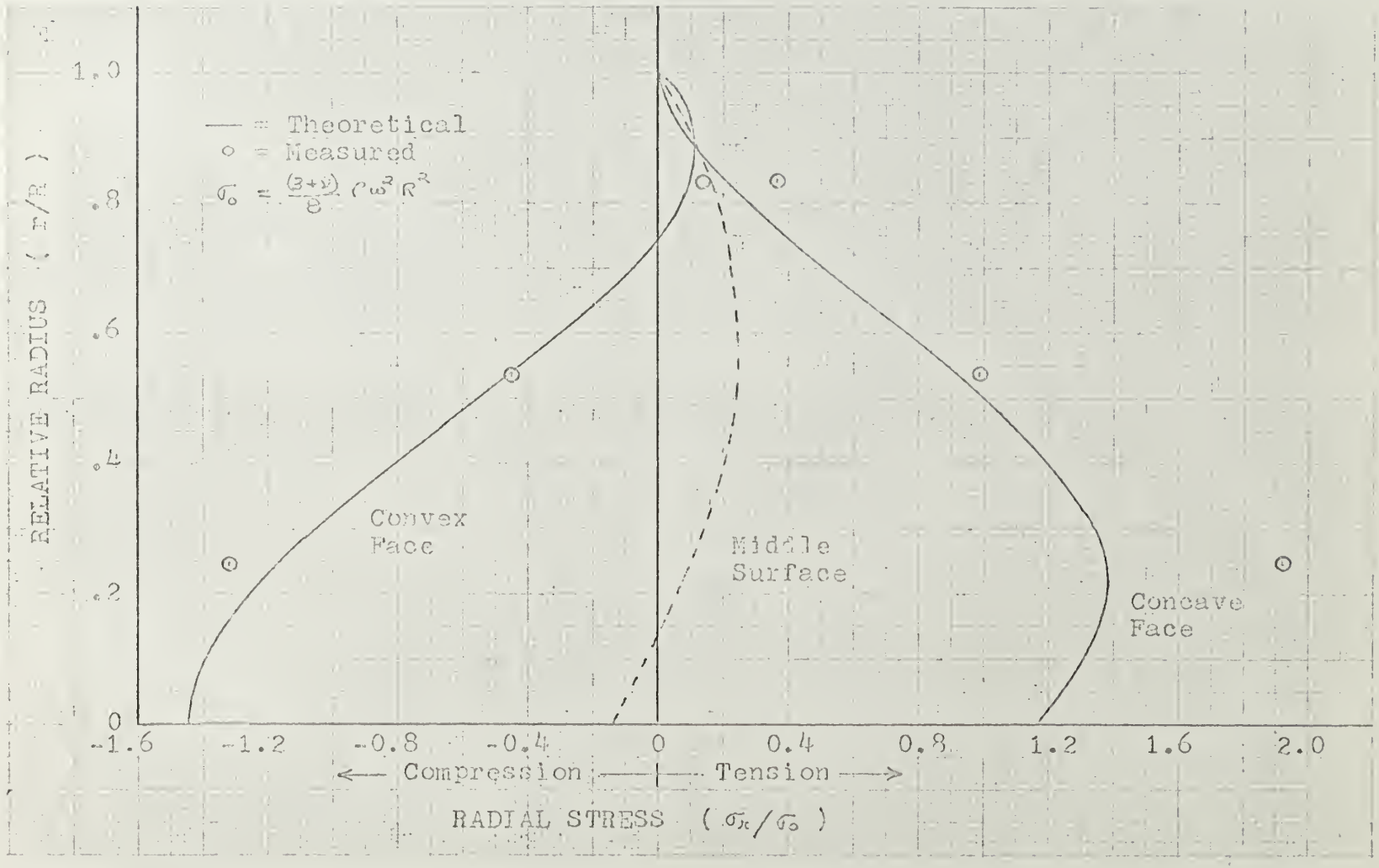


Fig. 15. Radial Stress in a Conical Disk

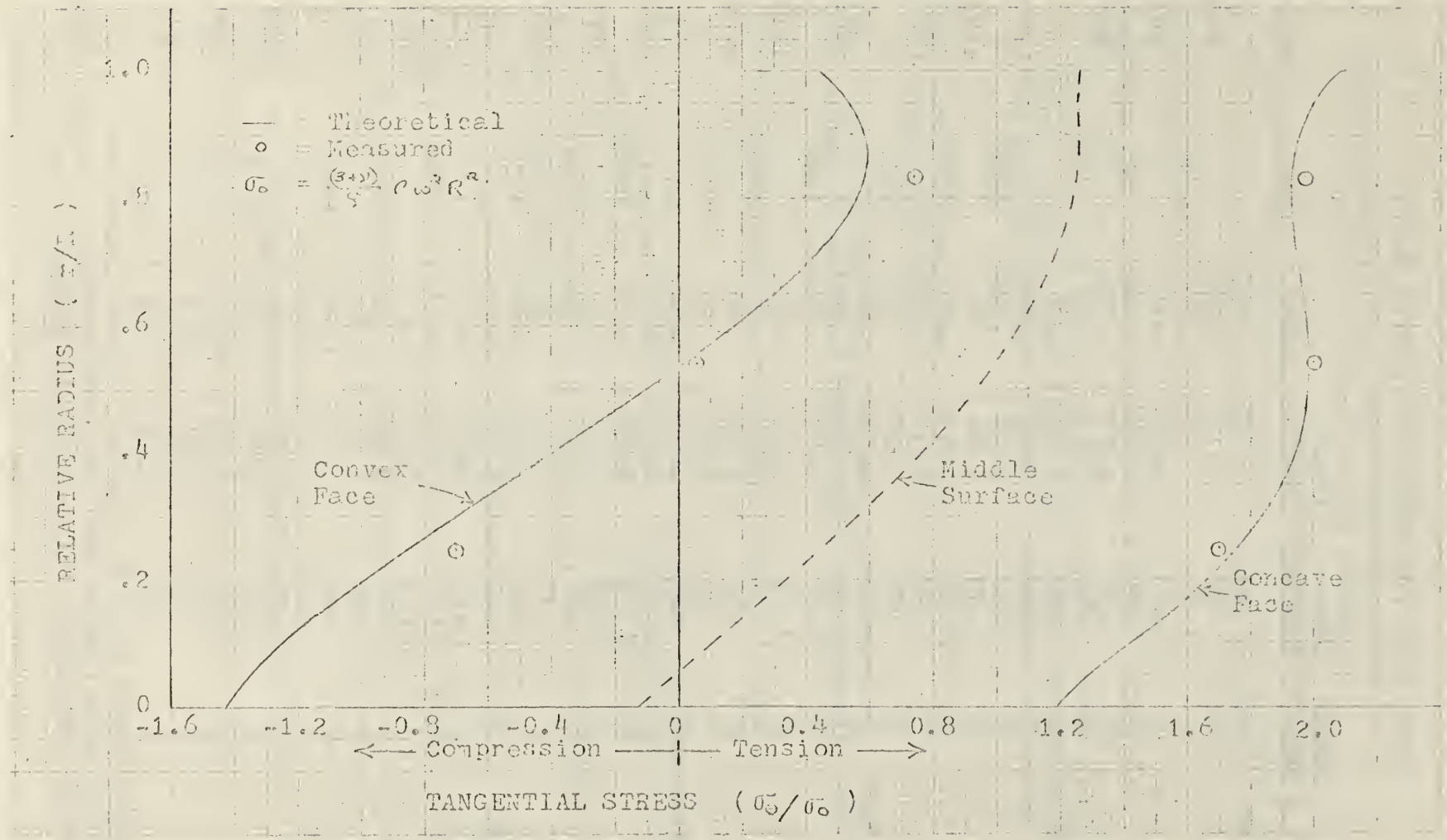


Fig. 16. Tangential Stress in a Conical Disk

TABLE I

Test Data for Symmetrical Disk Rotor

| RPM | Gage[1] Number | Zero Reading | Ave.[2] Reading | Δ mv | $\sigma_r$ | $\sigma_\theta$ |
|---|---|---|---|---|---|---|
| 5000 | 1 | .99 | 1.15 | .16 | | |
| | 3 | .99 | 1.19 | .20 | | 940 |
| | 4 | 1.22 | 1.38 | .16 | 842 | |
| | 5 | 1.03 | 1.21 | .18 | | 942 |
| | 6 | .96 | 1.18 | .22 | 921 | |
| | 7 | .97 | 1.17 | .20 | | 926 |
| | 8 | .96 | 1.11 | .15 | 805 | |
| 7500 | 1 | .99 | 1.33 | .34 | | |
| | 3 | .99 | 1.41 | .42 | | 1980 |
| | 4 | 1.22 | 1.56 | .34 | 1780 | |
| | 5 | 1.03 | 1.44 | .41 | | 2125 |
| | 6 | .96 | 1.45 | .49 | 2320 | |
| | 7 | .97 | 1.36 | .39 | | 1830 |
| | 8 | .96 | 1.27 | .31 | 1632 | |
| 10,000 | 1 | .99 | 1.59 | .60 | | |
| | 3 | .99 | 1.70 | .71 | | 3355 |
| | 4 | 1.22 | 1.80 | .58 | 3040 | |
| | 5 | 1.03 | 1.71 | .69 | | 3600 |
| | 6 | .96 | 1.80 | .84 | 3970 | |
| | 7 | .97 | 1.66 | .69 | | 3215 |
| | 8 | .96 | 1.49 | .53 | 2820 | |
| 12,500 | 1 | .99 | 1.99 | 1.00 | | |
| | 3 | .99 | 2.16 | 1.17 | | 5480 |
| | 4 | 1.22 | 2.14 | .92 | 4860 | |
| | 5 | 1.03 | 2.16 | 1.13 | | 4740 |
| | 6 | .96 | 2.35 | 1.39 | 6550 | |
| | 7 | .97 | 2.11 | 1.14 | | 5340 |
| | 8 | .96 | 1.85 | .89 | 4720 | |
| 15,000 | 1 | .99 | 2.41 | 1.41 | | |
| | 3 | .99 | 2.67 | 1.68 | | 8300 |
| | 4 | 1.22 | 2.55 | 1.33 | 6700 | |
| | 5 | 1.03 | 2.66 | 1.63 | | 8540 |
| | 6 | .96 | 2.96 | 2.00 | 9440 | |
| | 7 | .97 | 2.58 | 1.61 | | 7540 |
| | 8 | .96 | 2.22 | 1.26 | 6670 | |
| 17,500 | 1 | .99 | ---- | ---- | | |
| | 3 | .99 | 3.24 | 2.05 | | 9810 |
| | 4 | 1.22 | 3.00 | 1.78 | 9150 | |
| | 5 | 1.03 | 3.25 | 2.22 | | 11,600 |
| | 6 | .96 | 3.69 | 2.73 | 12,860 | |
| | 7 | .97 | 3.19 | 2.22 | | 10,370 |
| | 8 | .96 | 2.69 | 1.73 | 9170 | |

1. Gage Factor = 2.13
2. Three data points used for each average reading. These points had about one percent variation.

# APPENDIX A

## Computer Program for Centrifugal Stresses in a Rotor of Arbitrary Cross Section

The programming procedure for PROGRAM ROTOR is presented in a step by step outline so that an understanding of the analysis is unnecessary.

Consider the rotor cross section shown in Fig. 2.

Step 1. Select points n on the rotor boundary that are about equally spaced and best define the boundary. The maximum number of points that may be chosen is twenty five.

Step 2. Construct an imaginary boundary around the rotor cross section.

Step 3. Select points m on the imaginary boundary. The number of points m must equal the number of points n on the rotor.

Step 4. Determine the r and z coordinates of each point n and m.

Step 5. Determine the angles that the rotor surface makes with the radial direction. These angles must be recorded in fractions of $\pi$. $(0 \leq \gamma \leq 1.0)$

Step 6. Determine normal and tangential boundary stresses at each point n.

With the above information, prepare data cards. These are punched in the following format: (2F10.2, F10.4, 2F10.1, 2F10.2). The information on these cards is in the following order.

$r_n$ - The radial distance of each point n. (in.)

$z_n$ - The axial distance of each point n. (in.)

$\gamma_n$ - The angle $\gamma$ in fractions of $\pi$ .

$\sigma_{N_n}$ - The normal boundary stress at each point n. (psi)

$\tau_{T_n}$ - The tangential boundary stress at each point n. (psi)

$r_m$ - The radial distance of each point m. (in.)

$z_m$ - The axial distance of each point m. (in.)

Four other known constants are also punched on a single data card. This card has the following format: (I10, F10.0, F10.4, E10.1). The information on this card is in the following order.

n - The number of chosen points n.

$\omega$ - The angular velocity in revolutions per minute.

$\nu$ - Poisson's ratio.

$\rho$ - Rotor density.

# APPENDIX A

```
..JOB0168F,TROUTMAN,D.C. PROBLEM TIME 30 MINUTES
      PROGRAM ROTOR
      DIMENSION RN(25),ZN(25),XLMDA(25),RM(25),ZM(25),
     1 PARTR(25),PARTX(25),PARTZ(25),SIGR(25),SIGX(25),
     2 SIGZ(25),TAURZ(25),COEF(50,51),X(50),SIGB(25),TAUB(25),
     3 SIGRP(1250),SIGXP(1250),SIGZP(1250),TAURZP(1250),
     4 SIGRQ(1250),SIGXQ(1250),SIGZQ(1250),TAURZQ(1250)
      COMMON RN,ZN,XLMDA,RM,ZM,IND,II,JJ,XNU,COEF
      READ 9,NN,RPM,XNU,RHO
C     NN  = NUMBER OF POINTS N ON ROTOR BOUNDARY
C     RPM = ANGULAR VELOCITY IN REVOLUTIONS PER SECOND
C     XNU = POISSONS RATIO
C     RHO = ROTOR DENSITY
 9    FORMAT(I10,F10.0,F10.4,F10.3)
      PRINT 120,NN,RPM,XNU,RHO
 120  FORMAT(1H1,2X5H NN =I4,3X6H RPM =F10.0,3X6H XNU =F10.4,
     1 3X6H RHO =E10.3)
      PRINT 100
 100  FORMAT(//4X1HN,13X2HRN,13X2HZN,10X5HLAMDA,11X4HSIGB,11X4HTAUB,
     1 13X2HRM,13X2HZM)
      NXN = NN**2
      N2N = 2*NN
      READ 10,(RN(I),ZN(I),XLMDA(I),SIGB(I),TAUB(I),RM(I),ZM(I),I=1,NN)
C     RN  = RADIAL DISTANCE TO POINT N
C     ZN  = AXIAL DISTANCE TO POINT N
C     XLAMDA = ANGLE OF  OTOR SURFACE WRTO PLANE OF ROTATION
C     SIGB = NORMAL BOUNDARY STRESS
C     TAUB = TANGENTIAL BOUNDARY STRESS
C     RM  = RADIAL DISTANCE TO POINT M
C     ZM  = AXIAL DISTANCE TO POINT M
 10   FORMAT(2F10.2,F10.4,2F10.1,2F10.2)
      PRINT 200,(I,RN(I),ZN(I),XLMDA(I),SIGB(I),TAUB(I),RM(I),ZM(I),
     1 I = 1,NN)
```

```
      GO TO 20
3     SIGZP =-2.*SGP*AREA
      GO TO 20
4     TAURZP=-2.*SGP*AREA
      GO TO 20
5     SIGRQ = 2.*SGQ*AREA
      GO TO 20
6     SIGXQ = 2.*SGQ*AREA
      GO TO 20
7     SIGZQ = 2.*SGQ*AREA
      GO TO 20
8     TAURZQ =2.*SGQ*AREA
20    CONTINUE
      LL = 2*II-1
      KK = 2*II
C     SUBSTITUTE COMPONENTS INTO BOUNDARY STRESS EQUATIONS
      SUMP = (SIGRP +SIGZP)/2.
      DIFP = (SIGRP - SIGZP)/2.
      SIGNP = SUMP - DIFP*B - TAURZP*C
      TAUTP = - DIFP*C + TAURZP*B
C     GENERATE TERMS OF MATRIX WRTO P
      COEF(LL,JJ) = SIGNP
      COEF(KK,JJ) = TAUTP
C     SUBSTITUTE COMPONENTS INTO BOUNDARY STRESS EQUATIONS
      SUMQ = (SIGRQ + SIGZQ)/2.
      DIFQ = (SIGRQ - SIGZQ)/2.
      SIGNQ = SUMQ - DIFQ*B - TAURZQ*C
      TAUTQ = - DIFQ*C + TAURZQ*B
C     GENERATE TERMS OF MATRIX WRTO Q
      COEF(LL,JJ+NN) = SIGNQ
      COEF(KK,JJ+NN) = TAUTQ
C     STORE STRESS COMPONENTS
      SIGRP(JV) = SIGRP
      SIGXP(JV) = SIGXP
```

```
      SIGZP(JV) = SIGZP
      TAURZP(JV) = TAURZP
      SIGRQ(JV) = SIGRQ
      SIGXQ(JV) = SIGXQ
      SIGZQ(JV) = SIGZQ
      TAURZQ(JV) = TAURZQ
      JV = JV + 1
 30   CONTINUE
C     SUBSTITUTE COMPONENTS INTO BOUNDARY STRESS EQUATIONS
      SPART = (PARTR(II) + PARTZ(II))/2.
      DPART = (PARTR(II) - PARTZ(II))/2.
      PARTS = SPART - DPART*B
      PARTT = -DPART*C
C     GENERATE TERMS OF MATRIX WRTO BOUNDARY AND CENTRIFUGAL STRESSES
      COEF(LL,N2N+1) = SIGB(II) - PARTS
      COEF(KK,N2N+1) = TAUB(II) - PARTT
 40   CONTINUE
      PRINT 300
 300  FORMAT(1H1,4X5HSIGRP,9X5HSIGXP,9X5HSIGZP,8X6HTAURZP,
     1 9X5HSIGRQ,9X5HSIGXQ,9X5HSIGZQ,8X6HTAURZQ,7X1HJ)
      PRINT 400,(SIGRP(J),SIGXP(J),SIGZP(J),TAURZP(J),
     1 SIGRQ(J),SIGXQ(J),SIGZQ(J),TAURZQ(J),J,J = 1,NXN)
 400  FORMAT(/8E14.6,1I4)
      PRINT 600
 600  FORMAT(1H12X1HN,6X2HRN,8X2HZN,14X5HPARTR,15X5HPARTX,15X5HPARTZ)
      PRINT900,(J,RN(J),ZN(J),PARTR(J),PARTX(J),PARTZ(J),J = 1,NN)
 900  FORMAT(//I4,2F10.4,3F20.3)
C     SOLVE MATRIX
      CALL JORDAN(COEF,N2N,X)
      CALL TIME
      PRINT 350
 350  FORMAT(1H1,2X1HN,7X4HCOEF,1X4HX(N))
      PRINT 700,(N,X(N),N = 1,N2N)
 700  FORMAT(//1I4,1E18.8)
```

```
C       COMPUTE FINAL STRESSES
        DO 50 MM = 1,NN
        SRP = 0.0
        SXP = 0.0
        SZP = 0.0
        TRZP = 0.0
        L = 1
        I = (MM - 1)*NN + 1
        J = I
 60     SRP = SRP + X(L)*SIGRP(I)
        SXP = SXP + X(L) *SIGXP(I)
        SZP = SZP + X(L)*SIGZP(I)
        TRZP = TRZP +X(L)*TAURZP(I)
        L = L + 1
        I = I + 1
        IF(L - NN)60,60,70
 70     SRQ = 0.0
        SXQ = 0.0
        SZQ = 0.0
        TRZQ = 0.0
 80     SRQ = SRQ + X(L)*SIGRQ(J)
        SXQ = SXQ + X(L)*SIGXQ(J)
        SZQ = SZQ + X(L)*SIGZQ(J)
        TRZQ = TRZQ + X(L)*TAURZQ(J)
        L = L + 1
        J = J + 1
        IF(L - N2N)80,80,90
 90     SIGR(MM) = SRP + SRQ + PARTR(MM)
        SIGX(MM) = SXP + SXQ + PARTX(MM)
        SIGZ(MM) = SZP + SZQ + PARTZ(MM)
        TAURZ(MM) = TRZP + TRZQ
 50     CONTINUE
        CALL TIME
        PRINT 500
```

```
  500  FORMAT(1H13X1HN, 7X2HRN,10X2HZN,13X4HSIGR,11X4HSIGX,11X4HSIGZ,
     1 10X5HTAURZ)
       PRINT 800,(I,RN(I),ZN(I),SIGR(I),SIGX(I),SIGZ(I),TAURZ(I),
     1 I = 1,NN)
  800  FORMAT(//I4,2F12.4,4F15.3)
C      PROGRAM ROUGH CHECK
       DO 69 K = 1,NN
       SGR=(3.+XNU)/8.*RHO*RDPS**2*(144.-RN(K)**2)
       SGX=(3.+XNU)/8.*RHO*RDPS**2*144.-((1.+3.*XNU)/8.
     1*RHO*RDPS**2*RN(K)**2)
       PRINT 1000,K,SGR,SGX
  1000 FORMAT(/4H N =I2,4X6H SGR =F12.3,4X6H SGX =F12.3)
  69   CONTINUE
C      PROGRAM ROUGH CHECK TWO
       DO 79 KI=1,NN
       SGX2=(-.5*RHO*RDPS**2*RN(KI)**2)/(LOGF(ZN(KI))-LOGF(1.0))
       SGR2=(-.5*RHO*RDPS**2*RN(KI)**2)/(LOGF(ZN(KI))-LOGF(1.0))
       PRINT 2000,KI,SGR2,SGX2
  2000 FORMAT(/4H N =I2,4X6H SGR2=F12.3,4X6H SGX2=F12.3)
    79 CONTINUE
       END
       FUNCTION F(X)
       DIMENSION RN(25),ZN(25),XLMDA(25),RM(25),ZM(25),COEF(50,51)
       COMMON RN,ZN,XLMDA,RM,ZM,IND,II,JJ,XNU,COEF
       D = COSF(X)
       E = SINF(X)
       F0 = E**2
       F1 = RN(II)/RM(JJ)
       F2 = ((ZN(II)-ZM(JJ))/RM(JJ))
       F3=SQRTF((F1**2)+1.-2.*F1*D)
       F4=SQRTF((F1**2)+1.-2.*F1*D+F2**2)
       F5=F1*D-1.
       F6 = SQRTF((F1**2)*(F0)+F2**2)
       F7=(1.-2.*XNU)/F4**3
```

```
      F8 = F4**5
      F9 = F7*F5
      F10 = F9 -(3.*F5*(F6**3))/F8
      F11 = F9+(3.*(F5**3))/F8
      F12 = F7*F6+(3.*F6*(F5**2))/F8
      F13 = (F2**2)/(F6**2)
      F14 = F1/F6
      GO TO(1,2,3,4,5,6,7,8),IND
    1 F = F2*(F7-(3.*((F1-D)**2))/F8)
      RETURN
    2 F = F2*(F7-(3.*E**2)/F8)
      RETURN
    3 F =  (F2*(F7+(3.*F2**2)/F8))
      RETURN
    4 F =  (F7 + (3.*F2**2)/F8)*(F1 - COSF(X))
      RETURN
    5 F = ((F14**2)*(F0**2))*F10-2.*F14*F0*D*F12+F13*F0*F9-(D**2)*F11
      RETURN
    6 F = (F14**2)*F0*(D**2)*F10+2.*F14*F0*D*F12+F13*(D**2)*F9-F0*F11
      RETURN
    7 F = F13*F10+(F14**2)*F0*F9
      RETURN
    8 F15 = F1*F2*F0/F6**2
      F = F15*F10-F15*F9-F2*D*F12/F6
      RETURN
      END
C     D1 UCSD SIMCON
C     REVISED OCTOBER 1962
      SUBROUTINE SIMCON(X1,XEND,TEST,LIM,AREA,NOI,R)
      NOI=0
      R1=10.0
      ODD=0.0
      INT=1
      V=1.0
```

```
      EVEN=0.0
      AREA1=0.0
19    ENDS=F(X1)+F(XEND)
2     H=(XEND-X1)/V
      ODD=EVEN+ODD
      X=X1+H/2.
      EVEN=0.0
      DO 3 KI = 1,INT
21    EVEN=EVEN+F(X)
      X=X+H
3     CONTINUE
31    AREA=(ENDS+4.0*EVEN+2.0*ODD)*H/6.0
      NOI=NOI+1
34    R=ABSF((AREA1-AREA)/AREA)
      IF(NOI-LIM)341,35,35
341   IF(R-TEST)35,35,4
35    RETURN
4     AREA1=AREA
46    INT=2*INT
      V=2.0*V
      GO TO 2
      END
      SUBROUTINE JORDAN (A,N,X)
      DIMENSION A(50,51),X(50)
      K =N+1
      PRINT 69,((A(I,J),J=1,K), I=1,N)
   69 FORMAT (5E20.10)
11    IF (K-1)13,6,15
15    D=0.
      DO 2 I=2,K
      IF(ABSF(A(I-1,1))-D) 2,2,3
3     L =I-1
      D = ABSF(A(L,1))
2     CONTINUE
```

```
4       IF(L-1)5,6,5
5       DO 7 J=1,K
        D =A(L,J)
        A(L,J) = A(1,J)
7       A(1,J) = D
6       DO 8 I =1,N
8       X(I) = A(I,1)
        IF (K-1)12,13,12
12      DO 10 J=2,K
        D = A(1,J)/X(1)
        DO  9 I=2,N
9       A(I-1,J-1)  = A(I,J) -X(I)*D
10      A(N,J-1) =D
        K = K-1
        GO TO 11
13      CONTINUE
        RETURN
        END
        END
```

DATA

| | | | | | | |
|---|---|---|---|---|---|---|
| 14 | 20000. | .3333 | .720E-3 | | | |
| 1.00 | 1.00 | .0000 | .0 | .0 | 2.43 | 14.00 |
| 3.00 | 1.00 | .0000 | .0 | .0 | 7.29 | 14.00 |
| 5.00 | 1.00 | .0000 | .0 | .0 | 12.15 | 14.00 |
| 7.00 | 1.00 | .0000 | .0 | .0 | 16.92 | 13.16 |
| 9.00 | 1.00 | .0000 | .0 | .0 | 21.16 | 10.60 |
| 11.00 | 1.00 | .0000 | .0 | .0 | 24.28 | 6.67 |
| 12.00 | .5 | -0.5 | .0 | .0 | 25.92 | 2.29 |
| 12.00 | -.5 | -0.5 | .0 | .0 | 25.92 | -2.29 |
| 11.00 | -1.0 | -1.0 | .0 | .0 | 24.28 | -6.67 |
| 9.00 | -1.00 | -1.0 | .0 | .0 | 21.16 | -10.60 |
| 7.00 | -1.00 | -1.00 | .0 | .0 | 16.92 | -13.16 |
| 5.00 | -1.0 | -1.0 | .0 | .0 | 12.15 | -14.00 |
| 3.00 | -1.0 | -1.0 | .0 | .0 | 7.29 | -14.00 |
| 1.00 | -1.00 | -1.0 | .0 | .0 | 2.43 | -14.00 |

# APPENDIX B

## Evaluation of Material Properties

Tensile and torsional test specimens were machined from the same stock as the two test rotors. Fig. 17 contains the machinist's drawing for the tensile test specimen. The torsion test specimen was a one inch diameter bar.

A Riehle Model PS-300 Universal testing machine was used to test the tensile specimens. This machine prints a graph of load percentage versus strain, of which Fig. B-1 is a sample. The modulus of elasticity is calculated from the linear portion of the curve. A series of four specimens were tested and the values of E determined were

| Test No. | $E \times 10^6$ (psi) |
|---|---|
| 1 | 10.40 |
| 2 | 10.53 |
| 3 | 10.53 |
| 4 | 10.62 |

From these tests the average value of E was determined as

$$E = 10.5 \times 10^6 \text{ (psi)}$$

The torsion tests were conducted using the Tinius-Olsen torsion testing machine. The outputs of this machine are applied torque and angle of twist. From this information the modulus of rigidity is computed using the formula

$$G = \frac{TL}{J\theta}$$

where for a solid circular shaft

$$J = \frac{\pi D^4}{32}$$

The test data from two test runs is shown on Table B-I.

Values of modulus of rigidity obtained from these data were

| Test No. | $G \times 10^6$ (psi) |
|---|---|
| 1 | 3.94 |
| 2 | 3.94 |

which gives an average value of G as

$$G=3.94 \times 10^6 \text{ (psi)}$$

Poisson's ratio was calculated from the formula

$$\nu = \frac{E}{2G} - 1$$

which yielded as a value of Poisson's ratio for the rotor material

$$\nu = .335$$

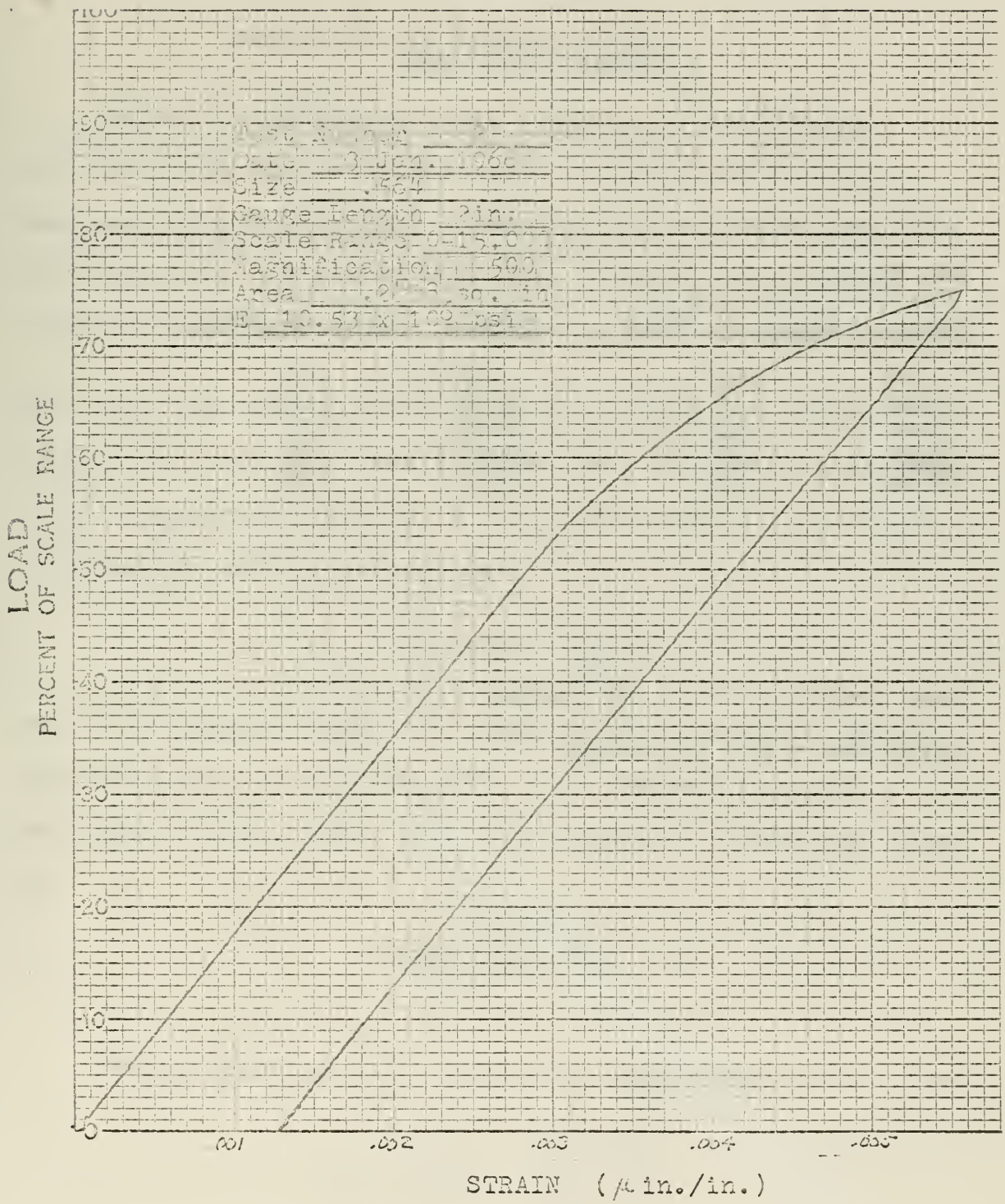


Fig. B-1. Stress-Strain Curve for Test Rotor Material

TABLE B-I

Torsion Test Data

| Run No. 1 | | Run No. 2 | |
|---|---|---|---|
| Torque | Angle of Twist | Torque | Angle of Twist |
| 0 | .01 | 0 | .05 |
| 1000 | .11 | 1000 | .16 |
| 2000 | .22 | 2000 | .27 |
| 3000 | .33 | 3000 | .39 |
| 4000 | .45 | 4000 | .50 |

Gage length = L = 3 5/8 inches

Lever arm = R = 12 inches

$$G = 3.94 \times 10^{6} \text{ (psi)}$$

# APPENDIX C

## Random errors of measurement

Using the method of least squares, it is desired to obtain the best straight line through a series of measured data points, and to determine a standard deviation of these data. Assuming that this straight line passes through the origin of x-y coordinates it is defined by

$$\bar{y} = mx$$

The best line can be obtained by minimizing the sum of squares of the deviations between the y values of this line and the measured y values, $y_i$, at each point n. This "sum of squares", $S^2$, is defined as

$$S^2 = \sum_{i=1}^{n} (y_i - \bar{y})^2 = \sum_{i=1}^{n} (y_i - mx)^2 \qquad (1)$$

and it is desired that this quantity be minimized. Taking the derivative of this quantity with respect to m and equating to zero, shows that the slope (m) of the best line is

$$m = \frac{\sum_{i=1}^{n} (y_i x_i)}{\sum_{i=1}^{n} x_i^2}$$

Substitution of this value of m into equation (1) gives

$$S^2 = \sum_{i=1}^{n} y_i^2 - \frac{\left[\sum_{i=1}^{n} y_i x_i\right]^2}{\sum_{i=1}^{n} x_i^2}$$

The degrees of freedom in this specific application are (n-1). The best estimate of the variance is given by

the expression

$$s^2 = \frac{S^2}{(n-1)}$$

The quantity (s) is then the estimated standard deviation.

Using this method, Table C-I summarizes these values for the data obtained from the hot spin unit.

TABLE C-I

Summary Of Random Errors Of Measurement

| Radius | Stress Direction | No. of Points | Slope | Sum of Squares |
|---|---|---|---|---|
| 1.5 | radial | 11 | .00383 | 344,782 |
| 1.5 | tangential | 10 | .00348 | 87,708 |
| 3.25 | radial | 20 | .00273 | 20,720 |
| 3.25 | tangential | 20 | .00310 | 985,180 |
| Mean Overall | | 61 | | 1,438,390 |

| Radius | Degrees of Freedom | Estimated Variance | Est. Std. Deviation | Std. Dev. Ref. Stress[1] |
|---|---|---|---|---|
| 1.5 | 10 | 34,478 | 185.5 | 1.43% |
| 1.5 | 9 | 9,745 | 98.5 | 0.77% |
| 3.25 | 19 | 1,090 | 32.5 | 0.35% |
| 3.25 | 19 | 51,851 | 225. | 2.16% |
| Mean Overall | 57 | 25,250 | 159. | 1.24% |

Mean Overall Standard Deviation of Strain[2]

$$= \frac{159}{10.5 \times 10^6} = 15.2 \times 10^{-6} \text{ in/in}$$

1. Reference Stress = 12,850 psi

2. $E = 10.5 \times 10^6$ psi

## APPENDIX D

Computer solution for centrifugal stresses in a conical rotor

This computer solution utilizes six term approximations to represent the stress functions $\Psi$ and $\chi$ of the general solution for the centrifugal stresses in a conical rotor.

This computer program as presented is for the specific case discussed in Part III of this report. Terms have been named to resemble as nearly as possible those used in the analysis. The results of this program are the radial and tangential surface stresses of the specified rotor. Radial distance increments of 0.25 inches and centrifugal speed increments of 1000 revolutions per minute have been utilized.

This program is easily adapted for computing the stresses in any conical rotor of interest. The following changes should be made to adapt the program to the rotor of concern.

| Line Number | Quantity to Change | Description |
|---|---|---|
| 5 | W | maximum rotor radius (in.) |
| 9 | RHO | mass density of rotor material |
| 10 | XNU | Poisson's ratio |
| 11 | ALFA | tangent of the cone angle |
| 12 | H | rotor thickness |

Possible additional desired changes might include line 6 to investigate centrifugal speeds greater than 15,000 rpm, line 42 for stresses at radii below 0.5 inches, lines 43 and 64 for radius increments other than 0.25 inches, and line 66 for stresses other than at 1000 rpm increments of centrifugal speed.

```
..JOB0168FTROUTMAN
      PROGRAM CONROT
      DIMENSION COEF(100,101),X(100)
      N2N=2
      RPM=1000.
      W=6.0
      DO 75 I=1,15
      RDPS=RPM*.10467
      RDPSQ=RDPS**2
      RHO=.000258
      XNU=.3352
      ALFA=.17633
      H=.5/.98481
      C1=12.*ALFA**2/H**2
      C2=12.*ALFA/H**2
      C3=(3.+XNU)*RHO*RDPS**2*H
      C4=ALFA
      C5=(1.+XNU)*C4
      A2=-C2*(1.-XNU)/1.5
      B2=(C4+C5)/1.5
      B3=((C4+C5/2.)/(1.5-1./6.))*A2
      A4=((-C2*B3*(.5-XNU/6.))+C1*A2/2.)/(.5+1./6.-1./24.)
      A3=(-C2*B2*(1.-XNU/2.)+C1)/(1.5-1./6.)
      CENT1=-C3/(1.5-1./6.)
      B5=((C4/6.+C5/24.)*A4)/(1./6.+1./24.-1./120.)
      A6=((-C2*(1./24.-XNU/120.))*B5+C1*A4/24.)/(1./24.+1./120.-1./720.)
      CENT2=CENT1*(C4/2.+C5/6.)/(1./2.+1./6.-1./24.)
      B4=((C4/2.+C5/6.)*A3)/(1./2.+1./6.-1./24.)
      CENT3=((CENT1*C1/6.)-C2*CENT2*(1./6.-XNU/24.))/(1./6.+1./24.-1./
     1120.)
      A5=((C1*A3/6.)-C2*B4*(1./6.-XNU/24.))/(1./6.+1./24.-1./120.)
      CENT4= (CENT3*(C4/24.+C5/120.))/(1./24.+1./120.-1./720.)
      B6=((C4/24.+C5/120.)*A5)/(1./24.+1./120.-1./720.)
      COEF(1,1)=W+(A3*W**3)/6.+(A5*W**5)/120.
      COEF(1,2)=(A2*W**2)/2.+(A4*W**4)/24.+(A6*W**6)/720.
```

```
      COEF(1,3)=(-CENT1*W**3)/6.+(-CENT3*W**5)/120.
      COEF(2,1)=(B2*W**2)/2.+(B4*W**4)/24.+(B6*W**6)/720.
      COEF(2,2)=W+(B3*W**3)/6.+(B5*W**5)/120.
      COEF(2,3)=(-CENT2*W**4)/24.+(-CENT4*W**6)/720.
      CALL JORDAN2(COEF,N2N,X)
      A1=X(1)
      B1=X(2)
      R=0.5
      DO 76 J=1,23
      PSI=A1*R+(A2*R**2/2.)*B1+(A3*R**3/6.)*A1+CENT1*R**3/6.+(A4*
     1R**4/24.)*B1+(A5*R**5/120.)*A1+CENT3*R**5/120.+(A6*R**6/720.)*B1
      CHI=B1*R+(B2*R**2/2.)*A1+(B3*R**3/6.)*B1+(B4*R**4/24.)*A1+CENT2
     1*R**4/24.+(B5*R**5/120.)*B1+(B6*R**6/720.)*A1+CENT4*R**6/720.
      PSIPR=A1+A2*R*B1+(3.*A3*R**2/6.)*A1+3.*CENT1*R**2/6.+(4.*A4*R**3
     1/24.)*B1+(5.*A5*R**4/120.)*A1+5.*CENT3*R**4/120.+(6.*A6*R**5
     2/720.)*B1
      CHIPR=B1+B2*R*A1+(3.*B3*R**2/6.)*B1+(4.*B4*R**3/24.)*A1+4.*
     1CENT2*R**3/24.+(5.*B5*R**4/120.)*B1+(6.*B6*R**5/720.)*A1+6.*
     2CENT4*R**5/720.
      TR=PSI/R
      TO=PSIPR+RHO*RDPS**2*R**2*H
      RMOM=CHI/R
      OMOM=CHIPR-PSI*C4
      SRTOP=TR/H+6.*RMOM/H**2
      SRBOT=TR/H-6.*RMOM/H**2
      SOTOP=TO/H+6.*OMOM/H**2
      SOBOT=TO/H-6.*OMOM/H**2
      PRINT120,RPM,R,SRTOP,SRBOT,SOTOP,SOBOT,RDPSQ
  120 FORMAT (7F15.2)
      R=R+0.25
   76 CONTINUE
      RPM=RPM+1000.
   75 CONTUNUE
      END
      END
```

INITIAL DISTRIBUTION LIST

| | | No. Copies |
|---|---|---|
| 1. | Defense DocumentationCenter<br>Cameron Station<br>Alexandria, Virginia 22314 | 20 |
| 2. | Library<br>U. S. Naval Postgraduate School<br>Monterey, California | 2 |
| 3. | Commander, Naval Air Systems Command<br>Department of the Navy<br>Washington, D. C. 20360 | 1 |
| 4. | Dr. Richard W. Bell<br>Chairman, Department of Aeronautics<br>U. S. Naval Postgraduate School<br>Monterey, California | 2 |
| 5. | Dr. Theodore H. Gawain<br>Department of Aeronautics<br>U. S. Naval Postgraduate School<br>Monterey, California | 2 |
| 6. | LT. Robert Lee Harshberger, USN<br>1132 Edson Avenue<br>Johnstown, Pennsylvania | 1 |
| 7. | LT. Darrell Clinton Troutman<br>Winside, Nebraska 68790 | 1 |

## DOCUMENT CONTROL DATA - R&D

*(Security classification of title, body of abstract and indexing annotation must be entered when the overall report is classified)*

| | |
|---|---|
| 1. ORIGINATING ACTIVITY *(Corporate author)*<br>United States Naval Postgraduate School<br>Monterey, California | 2a. REPORT SECURITY CLASSIFICATION<br>Unclassified<br>2b. GROUP |

3. REPORT TITLE

CENTRIFUGAL STRESSES IN CONICAL ROTORS AND ROTORS OF ARBITRARY CROSS SECTION

4. DESCRIPTIVE NOTES *(Type of report and inclusive dates)*

5. AUTHOR(S) *(Last name, first name, initial)*

Harshberger, Robert L. LT. USN
Troutman, Darrell C. LT. USN

| 6. REPORT DATE | 7a. TOTAL NO. OF PAGES | 7b. NO. OF REFS |
|---|---|---|
| May 1966 | 101 | 5 |

| | |
|---|---|
| 8a. CONTRACT OR GRANT NO. | 9a. ORIGINATOR'S REPORT NUMBER(S) |
| b. PROJECT NO. | |
| c. | 9b. OTHER REPORT NO(S) *(Any other numbers that may be assigned this report)* |
| d. | |

10. AVAILABILITY/LIMITATION NOTICES

| 11. SUPPLEMENTARY NOTES | 12. SPONSORING MILITARY ACTIVITY |
|---|---|
| | Naval Air Systems Command<br>Department of the Navy<br>Washington, D. C. |

13. ABSTRACT

Part I of this report evaluates a computer solution for the centrifugal stresses in rotors of arbitrary cross section, as proposed by LT. R. A. Johnson in 1965. This solution was found to be unstable and in its present form is unacceptable. (U)

Part II is an evaluation of the hot spin test unit of the United States Naval Postgraduate School. This facility was found capable of measuring strains with excellent accuracy. (U)

Part III presents a new and original analytical solution for the stresses in any conical rotor of constant thickness. The theoretically predicted stresses are found to be in close agreement with the measured values for the particular rotor tested. (U)

| 14. KEY WORDS | LINK A | | LINK B | | LINK C | |
|---|---|---|---|---|---|---|
| | ROLE | WT | ROLE | WT | ROLE | WT |
| Centrifugal stresses | | | | | | |
| Rotors | | | | | | |
| Conical rotors | | | | | | |
| Arbitrary rotors | | | | | | |
| Spin facilities | | | | | | |

INSTRUCTIONS

1. ORIGINATING ACTIVITY: Enter the name and address of the contractor, subcontractor, grantee, Department of Defense activity or other organization *(corporate author)* issuing the report.

2*a*. REPORT SECURITY CLASSIFICATION: Enter the overall security classification of the report. Indicate whether "Restricted Data" is included. Marking is to be in accordance with appropriate security regulations.

2*b*. GROUP: Automatic downgrading is specified in DoD Directive 5200.10 and Armed Forces Industrial Manual. Enter the group number. Also, when applicable, show that optional markings have been used for Group 3 and Group 4 as authorized.

3. REPORT TITLE: Enter the complete report title in all capital letters. Titles in all cases should be unclassified. If a meaningful title cannot be selected without classification, show title classification in all capitals in parenthesis immediately following the title.

4. DESCRIPTIVE NOTES: If appropriate, enter the type of report, e.g., interim, progress, summary, annual, or final. Give the inclusive dates when a specific reporting period is covered.

5. AUTHOR(S): Enter the name(s) of author(s) as shown on or in the report. Enter last name, first name, middle initial. If military, show rank and branch of service. The name of the principal author is an absolute minimum requirement.

6. REPORT DATE: Enter the date of the report as day, month, year; or month, year. If more than one date appears on the report, use date of publication.

7*a*. TOTAL NUMBER OF PAGES: The total page count should follow normal pagination procedures, i.e., enter the number of pages containing information.

7*b*. NUMBER OF REFERENCES: Enter the total number of references cited in the report.

8*a*. CONTRACT OR GRANT NUMBER: If appropriate, enter the applicable number of the contract or grant under which the report was written.

8*b*, 8*c*, & 8*d*. PROJECT NUMBER: Enter the appropriate military department identification, such as project number, subproject number, system numbers, task number, etc.

9*a*. ORIGINATOR'S REPORT NUMBER(S): Enter the official report number by which the document will be identified and controlled by the originating activity. This number must be unique to this report.

9*b*. OTHER REPORT NUMBER(S): If the report has been assigned any other report numbers *(either by the originator or by the sponsor)*, also enter this number(s).

10. AVAILABILITY/LIMITATION NOTICES: Enter any limitations on further dissemination of the report, other than those imposed by security classification, using standard statements such as:

(1) "Qualified requesters may obtain copies of this report from DDC."

(2) "Foreign announcement and dissemination of this report by DDC is not authorized."

(3) "U. S. Government agencies may obtain copies of this report directly from DDC. Other qualified DDC users shall request through _____."

(4) "U. S. military agencies may obtain copies of this report directly from DDC. Other qualified users shall request through _____."

(5) "All distribution of this report is controlled. Qualified DDC users shall request through _____."

If the report has been furnished to the Office of Technical Services, Department of Commerce, for sale to the public, indicate this fact and enter the price, if known.

11. SUPPLEMENTARY NOTES: Use for additional explanatory notes.

12. SPONSORING MILITARY ACTIVITY: Enter the name of the departmental project office or laboratory sponsoring *(paying for)* the research and development. Include address.

13. ABSTRACT: Enter an abstract giving a brief and factual summary of the document indicative of the report, even though it may also appear elsewhere in the body of the technical report. If additional space is required, a continuation sheet shall be attached.

It is highly desirable that the abstract of classified reports be unclassified. Each paragraph of the abstract shall end with an indication of the military security classification of the information in the paragraph, repreaented as *(TS)*, *(S)*, *(C)*, *or (U)*.

There is no limitation on the length of the abstract. However, the suggested length is from 150 to 225 words.

14. KEY WORDS: Key words are technically meaningful terms or short phrases that characterize a report and may be used as index entries for cataloging the report. Key words must be selected so that no security classification is required. Identifiers, such as equipment model designation, trade name, military project code name, geographic location, may be used as key words but will be followed by an indication of technical context. The assignment of links, roles, and weights is optional.

FIG. 17

| 14. KEY WORDS | LINK A | | LINK B | | LINK C | |
|---|---|---|---|---|---|---|
| | ROLE | WT | ROLE | WT | ROLE | WT |
| Centrifugal stresses | | | | | | |
| Rotors | | | | | | |
| Conical rotors | | | | | | |
| Arbitrary rotors | | | | | | |
| Spin facilities | | | | | | |

## INSTRUCTIONS

1. ORIGINATING ACTIVITY: Enter the name and address of the contractor, subcontractor, grantee, Department of Defense activity or other organization *(corporate author)* issuing the report.

2*a*. REPORT SECURITY CLASSIFICATION: Enter the overall security classification of the report. Indicate whether "Restricted Data" is included. Marking is to be in accordance with appropriate security regulations.

2*b*. GROUP: Automatic downgrading is specified in DoD Directive 5200.10 and Armed Forces Industrial Manual. Enter the group number. Also, when applicable, show that optional markings have been used for Group 3 and Group 4 as authorized.

3. REPORT TITLE: Enter the complete report title in all capital letters. Titles in all cases should be unclassified. If a meaningful title cannot be selected without classification, show title classification in all capitals in parenthesis immediately following the title.

4. DESCRIPTIVE NOTES: If appropriate, enter the type of report, e.g., interim, progress, summary, annual, or final. Give the inclusive dates when a specific reporting period is covered.

5. AUTHOR(S): Enter the name(s) of author(s) as shown on or in the report. Enter last name, first name, middle initial. If military, show rank and branch of service. The name of the principal author is an absolute minimum requirement.

6. REPORT DATE: Enter the date of the report as day, month, year; or month, year. If more than one date appears on the report, uae date of publication.

7*a*. TOTAL NUMBER OF PAGES: The total page count should follow normal pagination procedures, i.e., enter the number of pages containing information.

7*b*. NUMBER OF REFERENCES: Enter the total number of references cited in the report.

8*a*. CONTRACT OR GRANT NUMBER: If appropriate, enter the applicable number of the contract or grant under which the report was written.

8*b*, 8*c*, & 8*d*. PROJECT NUMBER: Enter the appropriate military department identification, such as project number, subproject number, system numbers, task number, etc.

9*a*. ORIGINATOR'S REPORT NUMBER(S): Enter the official report number by which the document will be identified and controlled by the originating activity. This number must be unique to this report.

9*b*. OTHER REPORT NUMBER(S): If the report has been assigned any other report numbers *(either by the originator or by the sponsor)*, also enter this number(s).

10. AVAILABILITY/LIMITATION NOTICES: Enter any limitations on further dissemination of the report, other than those imposed by security classification, using standard statements such as:

(1) "Qualified requesters may obtain copies of this report from DDC."

(2) "Foreign announcement and disseminstion of this report by DDC is not authorized."

(3) "U. S. Government agencies may obtsin copies of this report directly from DDC. Other qualified DDC users shall request through _____."

(4) "U. S. military agencies may obtain copies of this report directly from DDC. Other qualified users shall request through _____."

(5) "All distribution of this report is controlled. Qualified DDC users shall request through _____."

If the report has been furnished to the Office of Technical Services, Department of Commerce, for sale to the public, indicate this fact and enter the price, if known.

11. SUPPLEMENTARY NOTES: Use for additional explanatory notes.

12. SPONSORING MILITARY ACTIVITY: Enter the name of the departmental project office or laboratory sponsoring *(paying for)* the research and development. Include address.

13. ABSTRACT: Enter an abstract giving a brief and factual summary of the document indicative of the report, even though it may also appear elsewhere in the body of the technical report. If additional space is required, a continuation sheet shall be attached.

It is highly desirable that the abstract of classified reports be unclassified. Each paragraph of the abstract shall end with an indication of the military security classification of the information in the paragraph, represented as *(TS)*, *(S)*, *(C)*, *or (U)*.

There is no limitation on the length of the abstract. However, the suggested length is from 150 to 225 words.

14. KEY WORDS: Key words are technically meaningful terms or short phrases that characterize a report and may be used as index entries for cataloging the report. Key words must be selected so that no security classification is required. Identifiers, such as equipment model designation, trade name, military project code name, geographic location, may be used as key words but will be followed by an indication of technical context. The assignment of links, rules, and weights is optional.

FIG. 17

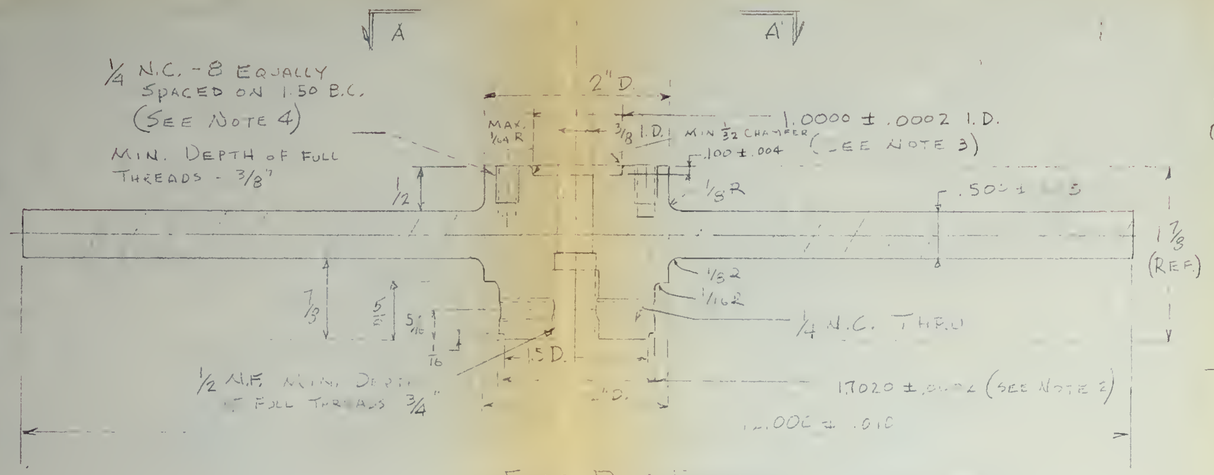


FLAT DISC ROTOR
(AL. ALLOY)

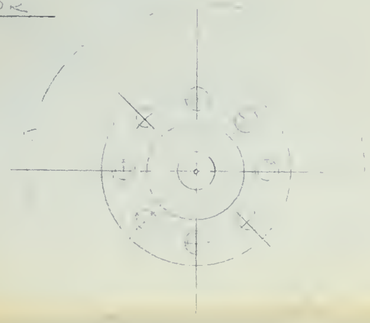

SECTION A-A

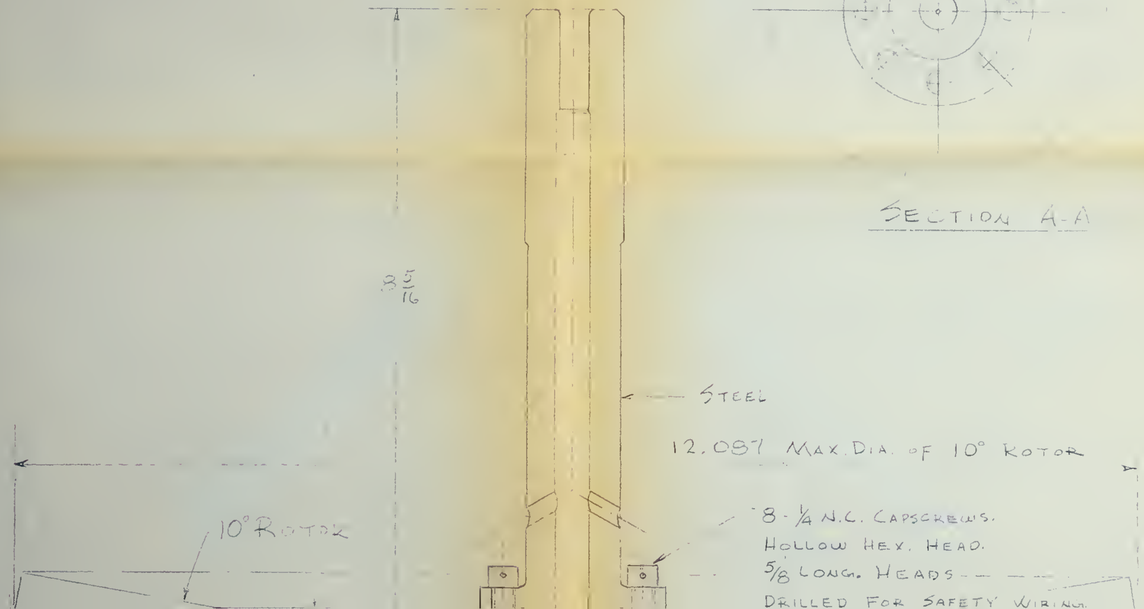


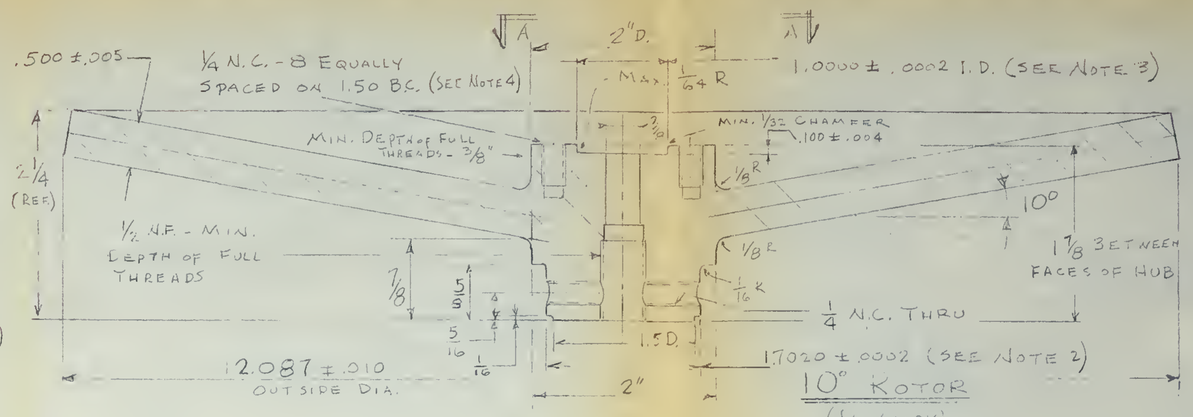


10" ROTOR
(AL. ALLOY)

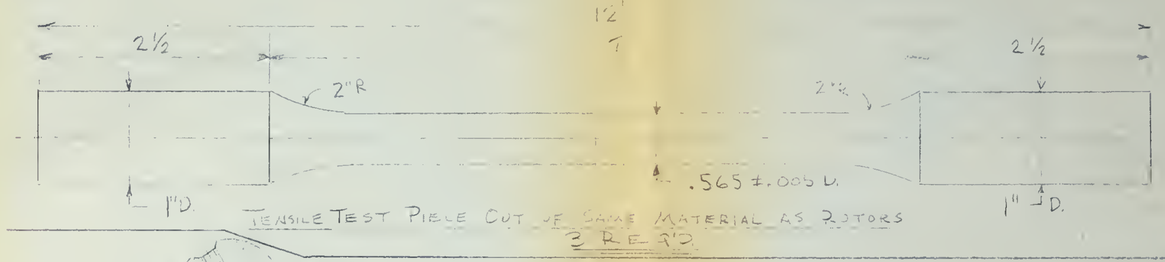


TENSILE TEST PIECE CUT OF SAME MATERIAL AS ROTORS
3 REQ'D.


SECTION C-C

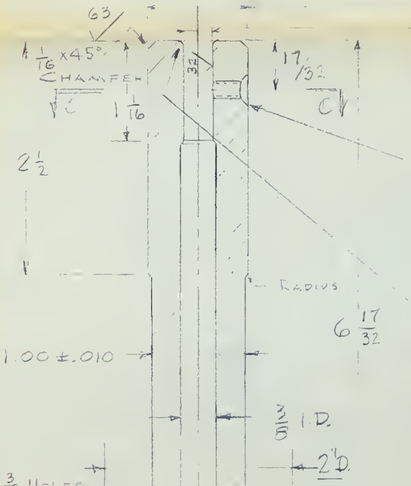


1.090 O.D. DIA.
.3128 - .313 I.D.

BORE TO BE CONCENTRIC WITH O.D. .003 T.I.R.

"C" TAP THRU, 3 HOLES EQUALLY SPACED. COUNTERSINK BOTH .220 ± .005 AT THE TWO OPPOSITE LOW POINTS SEE SECTION C-C ABOVE.

1/16 RAD. +.030 -.010 IT IS IMPORTANT THAT THIS RADIUS IS SMOOTH AND BLENDS OR FAIRS INTO BORE WITH NO RIDGE OR UNDERCUT. POLISH IF NECESSARY.

## NOTES

1. TOLERANCE WILL BE MET IF LIGHT PUSH FIT WITH PART TO BE SUPPLIED WITH THIS PRINT
2. TOLERANCE WILL BE MET IF LIGHT PUSH FIT BETWEEN STEEL PIECE AND EACH AL. DISC.
3. USE STEEL PC. AS TEMPLATE FOR LOCATING 8, 1/4 TAPPED HOLES IN DISCS (OR OTHERWISE INSURE EXACT MATCHING OF TAPPED & DRILLED HOLES.)
4. REMOVE ALL BURRS AND SHARP EDGES.

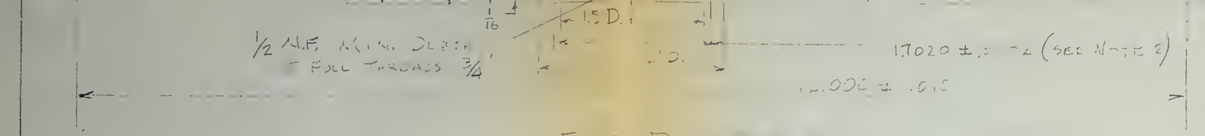


FLAT DISC ROTOR
(AL. ALLOY)

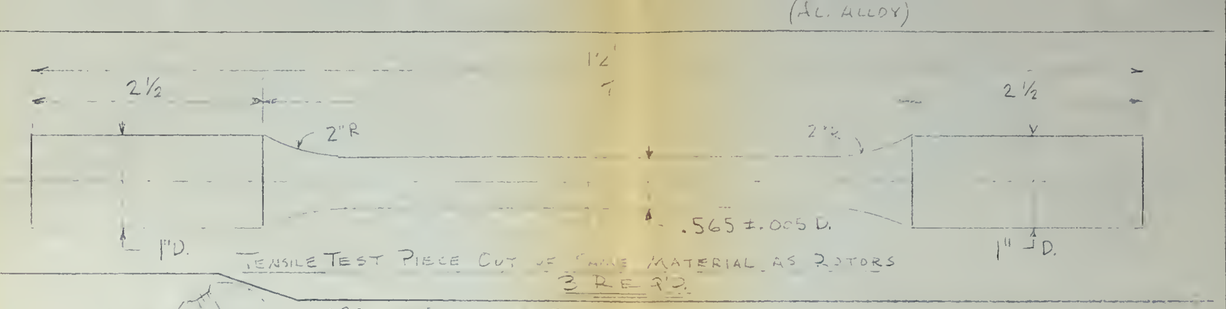


TENSILE TEST PIECE CUT OF SAME MATERIAL AS ROTORS
3 REQ'D.

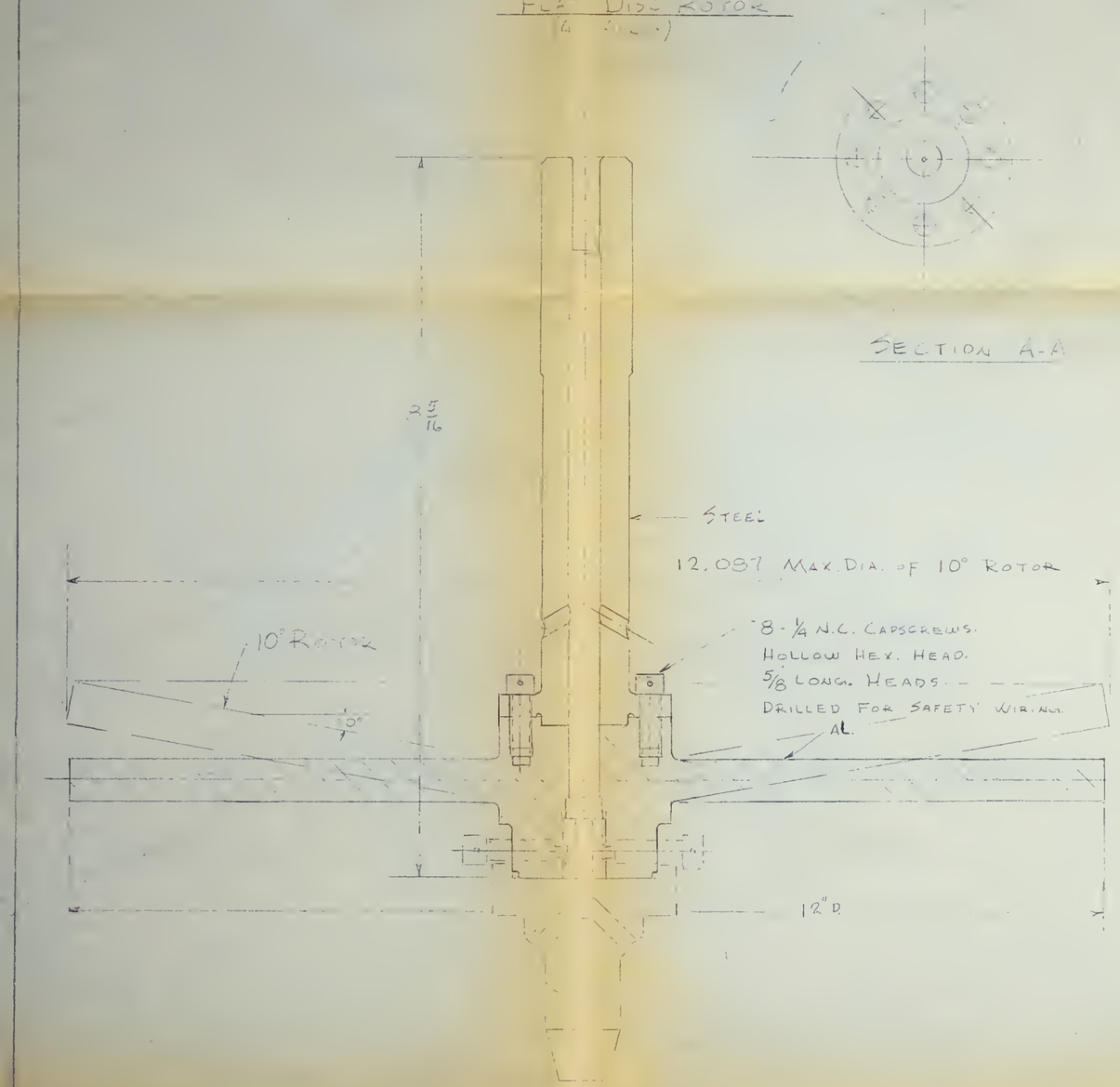


SECTION A-A

STEEL EXTENSION PIECE
(MILD STEEL)

## NOTES

1. TOLERANCE WILL BE MET IF LIGHT PUSH FIT WITH PART TO BE SUPPLIED WITH THIS PRINT
2. TOLERANCE WILL BE MET IF LIGHT PUSH FIT BETWEEN STEEL PIECE AND EACH AL. DISC.
3. USE STEEL PC. AS TEMPLATE FOR LOCATING 3, 1/4" TAPPED HOLES IN DISCS (OR OTHERWISE INSURE EXACT MATCHING OF TAPPED & DRILLED HOLES.)
4. REMOVE ALL BURRS AND SHARP EDGES.

| TEST ROTORS HOT SPIN RIG | 1192 |
|---|---|
| DRAWN M.R. Reynolds 8.'65 | APPROVED T.H. Sarpkaya 12/14/65 |

U. S. NAVAL POSTGRADUATE SCHOOL
DEPT. OF AERONAUTICS
MONTEREY, CALIFORNIA